13

Baryon Number Violation

Conveners: K.S. Babu, E. Kearns

U. Al-Binni, S. Banerjee, D. V. Baxter, Z. Berezhiani, M. Bergevin, S. Bhattacharya, S. Brice, R. Brock, T. W. Burgess, L. Castellanos, S. Chattopadhyay, M.-C. Chen, E. Church, C. E. Coppola, D. F. Cowen, R. Cowsik, J. A. Crabtree, H. Davoudiasl, R. Dermisek, A. Dolgov, B. Dutta, G. Dvali, P. Ferguson, P. Fileviez Perez, T. Gabriel, A. Gal, F. Gallmeier, K. S. Ganezer, I. Gogoladze, E. S. Golubeva, V. B. Graves, G. Greene, T. Handler, B. Hartfiel, A. Hawari, L. Heilbronn, J. Hill, D. Jaffe, C. Johnson, C. K. Jung, Y. Kamyshkov, B. Kerbikov, B. Z. Kopeliovich, V. B. Kopeliovich, W. Korsch, T. Lachenmaier, P. Langacker, C.-Y. Liu, W. J. Marciano, M. Mocko, R. N. Mohapatra, N. Mokhov, G. Muhrer, P. Mumm, P. Nath, Y. Obayashi, L. Okun, J. C. Pati, R. W. Pattie, Jr., D. G. Phillips II, C. Quigg, J. L. Raaf, S. Raby, E. Ramberg, A. Ray, A. Roy, A. Ruggles, U. Sarkar, A. Saunders, A. Serebrov, Q. Shafi, H. Shimizu, M. Shiozawa, R. Shrock, A. K. Sikdar, W. M. Snow, A. Soha, S. Spanier, G.C. Stavenga, S. Striganov, R. Svoboda, Z. Tang, Z. Tavartkiladze, L. Townsend, S. Tulin, A. Vainshtein, R. Van Kooten, C. E. M. Wagner, Z. Wang, B. Wehring, R. J. Wilson, M. Wise, M. Yokoyama, A. R. Young

13.1 Overview

Baryon Number, $\mathcal{B}$, is observed to be an extremely good symmetry of Nature. The stability of ordinary matter is attributed to the conservation of baryon number. The proton and the neutron are assigned $\mathcal{B} = +1$, while their antiparticles have $\mathcal{B} = -1$, and the leptons and antileptons all have $\mathcal{B} = 0$. The proton, being the lightest of particles carrying a non-zero $\mathcal{B}$, would then be absolutely stable if $\mathcal{B}$ is an exactly conserved quantum number. Hermann Weyl formulated the principle of conservation of baryon number in 1929 primarily to explain the stability of matter [1]. Weyl's suggestion was further elaborated by Stueckelberg [2] and Wigner [3] over the course of the next two decades. The absolute stability of matter, and the exact conservation of $\mathcal{B}$, however, have been questioned both on theoretical and experimental grounds. Unlike the stability of the electron which is on a firm footing as a result of electric charge conservation (electron is the lightest electrically charged particle), the stability of proton is not guaranteed by an analogous "fundamental" symmetry. Electromagnetic gauge invariance which leads to electric charge conservation is a true local symmetry with an associated gauge boson, the photon, while baryon number is only a global symmetry with no associated mediator.

If baryon number is only an approximate symmetry which is broken by small amounts, as many leading theoretical ideas elaborated here suggest, it would have a profound impact on our understanding of the evolution of the Universe, both in its early history and its late–time future. Violation of baryon number is an essential ingredient for the creation of an asymmetry of matter over antimatter in a symmetrical Universe that emerged from the Big Bang [4]. This asymmetry is a critical ingredient in modern cosmology, and is the primary driving force for the formation of structures such as planets, stars, and galaxies, and for the origin of everything they support. Even tiny violations of baryon number symmetry would impact the late–time future of the Universe profoundly. $\mathcal{B}$ violation would imply the ultimate instability of the proton and the

nucleus, which in turn would predict the instability of atoms, molecules, planets and stars, albeit at a time scale of the order of the lifetime of the proton [5].

There are many theoretical reasons to believe that baryon number is perhaps not an exact symmetry of Nature. The Standard Model of particle physics is constructed in such a way that $\mathcal{B}$ is an accidental symmetry of the Lagrangian. This is true only at the classical level, however. Quantum effects associated with the weak interactions violate baryon number non-perturbatively [6, 7]. These violations arise because $\mathcal{B}$ is anomalous with respect to the weak interactions. While such violations are so small as to be unobservable (at zero temperature), owing to exponential suppression factors associated with tunneling rates between vacuua of differing baryon number, as a matter of principle these tiny effects imply that the minimal Standard Model already has $\mathcal{B}$ violation. It is noteworthy that the same $\mathcal{B}$–violating interactions at high temperature become unsuppressed, when tunneling between vacuua may be replaced by thermal fluctuations which allow crossing of the barriers [8, 9]. It is these high temperature $\mathcal{B}$–violation of the Standard Model that enables a primordial lepton asymmetry generated via leptogenesis [10]– a popular mechanism for generating matter asymmetry – to be converted to baryon asymmetry of the Universe.

Within the framework of the Standard Model itself, one can write down higher dimensional operators suppressed by inverse powers of a mass scale assumed to be much larger than the W and Z boson masses. Such non-renomrmalizable operators which are fully compatible with the gauge invariance of the Standard Model indeed lead to baryon number violation at dimension 6, with a suppression factor of two inverse powers of a heavy mass scale [11, 12, 13]. What could be the origin of such non-renormalizable operators? One possible source is quantum gravity [14, 15, 16, 17]. It is suspected strongly that quantum gravity will not respect any global symmetry such as baryon number. $\mathcal{B}$ violating dimension 6 operators arising from quantum gravity effects would lead to proton decay, but with a long lifetime estimated to be of order 10^{44} yrs., which is well beyond the sensitivity of ongoing and near-future experiments. Nevertheless, this is a further illustration of non-exactness of baryon number symmetry.

In Grand Unified Theories [18, 19], GUTs for short, which are well motivated on several grounds, baryon number is necessarily violated, and the proton must decay, albeit with a long lifetime exceeding 10^{30} yrs. These theories unify the strong, weak and electromagnetic forces into a single unified force. Simultaneously these theories also unify quarks with leptons, and particles with antiparticles. Most remarkably, the unification of the three gauge couplings predicted by GUTs [20] is found to hold, in the context of low energy supersymmetry, at an energy scale of about 10^{16} GeV. Particles with masses at such a large energy scale (amounting to distance scale of order 10^{-30} cm) are beyond reach of direct production by accelerators. Nevertheless, the idea of grand unification lends itself to experimental test in proton decay, with the partial lifetime predicted to lie in the range of $10^{30} - 10^{36}$ yrs. for the dominant decay modes $p \to \overline{\nu} K^+$ and $p \to e^+\pi^0$. These predictions are within reach of ongoing and forthcoming experiments. While proton decay is yet to be seen, the grand unification idea has turned out to be spectacularly successful as regards its other predictions and postdictions. These include an understanding of electric charge quantization, the co-existence of quarks and leptons and their quantum numbers, and a natural explanation of the scale of neutrino mass. Proton decay now remains as a key missing piece of evidence for grand unification.

One can in fact argue, within a class of well-motivated ideas on grand unification, that proton decay should occur at accessible rates, with a lifetime of about 10^{35} years, for protons decaying into $e^+\pi^0$, and a lifetime of less than a few $\times 10^{34}$ years for protons decaying into $\overline{\nu} K^+$. The most stringent limits on proton lifetimes now come from Super-Kamiokande [21]. It is a remarkable scientific achievement that this experiment, along with some of its predecessors, has improved the lifetime limit by many orders of magnitude compared to the pioneering experiment of Reines, Cowan and Goldhaber of 1954 [22]. For the two important decay modes mentioned above, the SuperKamiokande limits are [21]:

$$\tau(p \to e^+\pi^0) > 1.4 \times 10^{34} \text{ yrs}, \qquad \tau(p \to \bar{\nu} K^+) > 5.9 \times 10^{33} \text{ yrs}. \tag{13.1}$$

These well-motivated models then predict the observation of proton decay if one can improve the current sensitivity (of Super-Kamiokande) by a factor of five to ten. This is why an improved search for proton decay, possible only with a large underground detector, is now most pressing.

There is another promising way of testing the violation of baryon number, in the spontaneous conversion of neutrons into antineutrons [23, 24, 25]. This process – neutron–antineutron oscillation – is analogous to $K^0 - \overline{K}^0$ mixing in the meson sector which violates strangeness by two units. In neutron–antineutron ($n - \overline{n}$) oscillations $\mathcal{B}$ is violated by two units. Thus these oscillations, if discovered, would test a different sector of the underlying theory of baryon number violation compared to proton decay searches which would be sensitive to the $|\Delta\mathcal{B}| = 1$ sector.

There are several motivations to carry out $n - \overline{n}$ oscillation searches to the next level of experimental sensitivity. In the Standard Model when small neutrino masses are accommodated via the seesaw mechanism, lepton number ($\mathcal{L}$) gets violated by two units. Since the weak interactions violate $\mathcal{B}$ and $\mathcal{L}$ separately at the quantum level, but conserve the difference $\mathcal{B} - \mathcal{L}$, neutrino Majorana mass induced by the seesaw mechanism is suggestive of an accompanying $\Delta\mathcal{B} = 2$ interactions, so that $\Delta(\mathcal{B} - \mathcal{L}) = 0$ is preserved. Secondly, the interactions that lead to $n - \overline{n}$ oscillations may also be responsible for the generation of the baryon asymmetry of the Universe. Unlike the leading proton decay modes $p \to e^+\pi^0$ and $p \to \overline{\nu}K^+$, which violate $\mathcal{B}$ and $\mathcal{L}$ by one unit, but preserve $\mathcal{B} - \mathcal{L}$ symmetry, $n - \overline{n}$ oscillations violate $\mathcal{B} - \mathcal{L}$ by two units. The primordial baryon asymmetry induced by interactions causing such oscillations would survive non-perturbative weak interaction effects, unlike the ones responsible for the leading modes of proton decay. There may thus be an intimate connection between $n - \overline{n}$ oscillations and the observed baryon asymmetry of the Universe [26]. Thirdly, unlike the $|\Delta\mathcal{B}| = 1$ operator which results in proton decay, the effective operators responsible for $n - \overline{n}$ oscillations have dimension 9, and are suppressed by five powers of an inverse mass scale. Consequently, an observation of $n - \overline{n}$ oscillation in the next round of experiments would suggest a relatively low scale of new physics, of order $10^3 - 10^5$ GeV. This would be quite contrary to the grand desert hypothesis. It should be noted that well motivated quark–lepton unified theories which implement the seesaw mechanism for neutrino masses at low energy scales do lead to observable $n - \overline{n}$ oscillation amplitude [26, 27, 28, 29, 30, 31, 32, 33, 34, 35, 36, 37].

$n - \overline{n}$ oscillation searches have been performed in the past, both with free neutron beams, and within nuclear environment in large underground detectors. The best limit on the characteristic time of oscillation derived from free neutron beam is $\tau_{n-\overline{n}} > 0.86 \times 10^8$ sec. from the ILL experiment at Grenoble [38]. The experimental signature of antineutron annihilation in a free neutron beam is spectacular enough that an essentially background free search is possible. An optimized experimental search for oscillations using free neutrons from a 1 MW spallation target at Fermilab's Project X can improve existing limits on the free neutron oscillation probability by *4 orders of magnitude*. This can be achieved by fully exploiting new slow neutron source and optics technology developed for materials science in an experiment delivering a slow neutron beam through a magnetically-shielded vacuum to a thin annihilation target. A null result at this level, when interpreted as $n - \overline{n}$ transition in nuclear matter, would represent the most stringent limit on matter instability with a lifetime exceeding 10^{35} yrs. Combined with data from the LHC and other searches for rare processes, a null result could also rule out a class of models where baryogenesis occurs below the electroweak phase transition.

13.2 Grand Unification and Proton Decay

The most compelling reason for the continued search for proton decay is perhaps the predictions of grand unified theories [18, 19], which unify the strong, weak and electromagnetic forces into a single underlying force. The apparent differences in the strengths of these interactions is explained by the running of the

coupling constants with momentum [20]. When the three measured gauge couplings are extrapolated from low energy to higher energies within the context of the Standard Model particle content, they tend to merge to a common value, but the three do not quite meet (see Fig. 13-1, left panel.) With the assumption of low energy supersymmetry, motivated independently by the naturalness of the Higgs boson mass, the three gauge couplings are found to unify nicely at a scale $M_{\rm GUT} \approx 2 \times 10^{16}$ GeV (see Fig. 13-1, right panel). This remarkable feature may be argued as a strong hint in favor of grand unification as well as supersymmetry.

GUTs explain many of the puzzling features observed in Nature that are not explained by the Standard Model. A prime example is the quantization of electric charge, together with $Q_{\rm proton} = -Q_{\rm electron}$ (to better than 1 part in 10^{21}). This is a natural consequence of grand unification, but not of the Standard Model, owing to the non-Abelian nature of the GUT symmetry, which leads to traceless generators and thus $Q_{\rm proton} + Q_{\rm electron} = 0$. The co-existence of quarks with leptons is explained in GUTs which in fact unify these two types of particles. The miraculous cancellation of chiral anomalies that occurs among each family of quarks and leptons has a symmetry–based explanation in GUTs. Furthermore, GUTs provide a natural understanding of the quantum numbers of quarks and leptons. Certain grand unified theories, notably those based on the gauge symmetry $SO(10)$ [39], require the existence of right-handed neutrinos, one per family, which play an essential role in the seesaw mechanism for generating small Majorana masses for the ordinary neutrinos. These right-handed neutrinos also may be responsible for the generation of the baryon asymmetry of the Universe via leptogenesis [10]. The grouping of quarks with leptons, and particles with antiparticles, in a common GUT multiplet leads to the violation of baryon number and proton decay [18, 19]. The unification scale of $M_{\rm GUT} \approx 2 \times 10^{16}$ GeV of SUSY GUTs will serve as the benchmark for proton lifetime estimate.

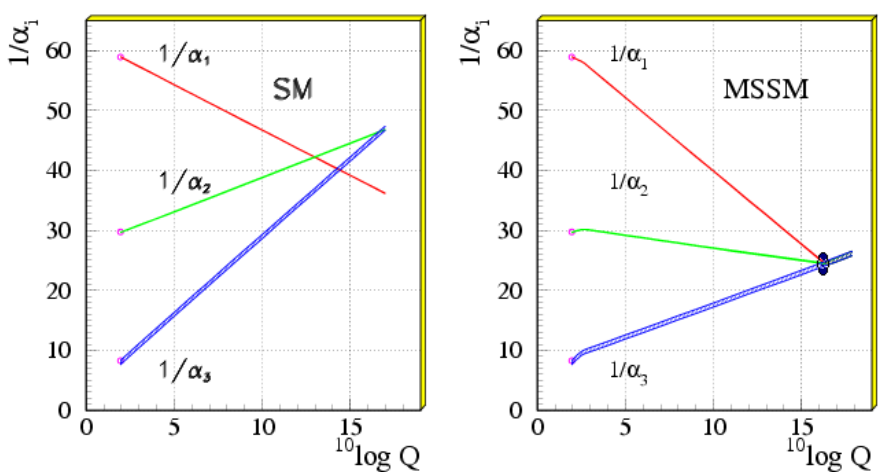

Figure 13-1. *Evolution of the three gauge couplings α_i with momentum Q: Standard Model (left panel) and Minimal Supersymmetric Standard Model (right panel)*

13.2.1 $SU(5)$ Unification and Proton Decay

$SU(5)$ is the simplest grand unified symmetry that contains the Standard Model gauge symmetry as a subgroup [19]. It turns out to be the most predictive as regards proton lifetime as well. This is because of small GUT scale threshold effects arising from the superheavy sector of the theory. The masses of these particles, which are the left-over Higgs bosons from the GUT symmetry breaking, are not precisely determined from the extrapolation of low energy gauge couplings. Their precise masses affect the determination of the

masses of X and Y gauge bosons of $SU(5)$, which are the mediators of proton decay. $SU(5)$ being the smallest GUT group has the smallest number of such supeheavy particles, and thus the least amount of uncertainty in proton lifetime estimate. The minimal non-supersymmetric version of $SU(5)$ [19] has already been excluded by the experimental lower limit on $p \to e^+\pi^0$ lifetime and the mismatch of the three gauge couplings when extrapolated to high energies (see left panel of Fig. 13-1). With low energy supersymmetry, which is independently motivated by the naturalness of the Higgs boson mass, there is a simple explanation why the decay $p \to e^+\pi^0$ has not been observed. The unification scale, and hence the mass of the X and Y gauge boson that mediate proton decay, increase significantly with low energy SUSY (see right panel of Fig. 13-1) [40].

Supersymmetric grand unified theories (SUSY GUTs) [41, 42, 43, 44, 45, 46, 47] are natural extensions of the Standard Model that preserve the attractive features of GUTs noted above, such as quantization of electric charge, and lead to reasonably precise unification of the three gauge couplings. They also explain the existence of the weak scale, which is much smaller than the GUT scale, and provide a dark matter candidate in the form of the lightest SUSY particle. Low energy SUSY brings in a new twist to proton decay, however, as it predicts a new decay mode $p \to \overline{\nu}K^+$ that would be mediated by the colored Higgsino [48],[49], the GUT/SUSY partner of the Higgs doublets (see Fig. 13-2, right panel). The lifetime for this mode in minimal renormalizable SUSY $SU(5)$ is typically shorter than the current experimental lower limit quoted in Eq. (13.1), provided that the SUSY particle masses are less than about 3 TeV, so that they are within reach of the LHC. This is, however, not the case in fully realistic SUSY $SU(5)$ models, as shall be explained below.

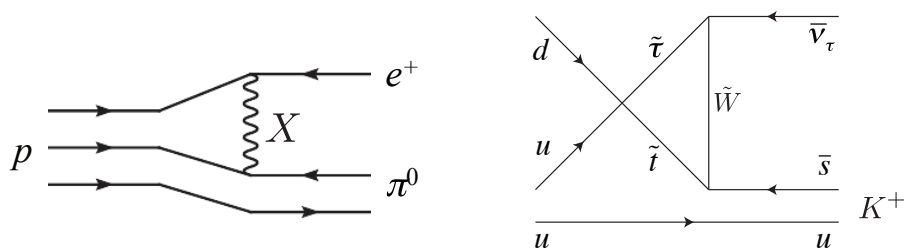

Figure 13-2. *Diagrams inducing proton decay in GUTs. $p \to e^+\pi^0$ mediated by X gauge boson (left) in non-SUSY and SUSY GUTs, and $p \to \overline{\nu}K^+$ generated by a $d = 5$ operator in SUSY GUTs. (right).*

In order to evaluate the lifetimes for the $p \to \overline{\nu}K^+$ and $p \to e^+\pi^0$ decay modes in SUSY $SU(5)$ [50], a symmetry breaking sector and a consistent Yukawa coupling sector must be specified. In $SU(5)$, one family of quarks and leptons is organized as $\{10 + \overline{5} + 1\}$, where $10 \supset \{Q, u^c, e^c\}, \overline{5} \supset \{d^c, L\}$, and $1 \sim \nu^c$. $SU(5)$ contains 24 gauge bosons, 12 of which are the gluons, $W^\pm, Z^0$ and the photon, while the remaining 12 are the (X, Y) bosons that transform as $(3, 2, -5/6)$ under $SU(3)_c \times SU(2)_L \times U(1)_Y$ and their conjugates. These bosons have both diquark and leptoquark couplings, which lead to baryon number violating processes. The diagram leading to the decay $p \to e^+\pi^0$ is shown in Fig. 13-2, left panel. $SU(5)$ breaks down to the Standard Model symmetry in the supersymmetric limit by employing a 24_H Higgs boson. Additionally, a $\{5_H + \overline{5}_H\}$ pair of Higgs bosons is employed, for electroweak symmetry breaking and the generation of quark and lepton masses. These fields contain the MSSM Higgs fields H_u and H_d. They also contain color-triplet fields (T and $\overline{T}$) with baryon number violating interactions. T and $\overline{T}$ must then have a GUT scale mass, while H_u and H_d from the same GUT multiplet must have weak scale masses. This is done in minimal SUSY $SU(5)$ by a fine-tuning, which is perhaps an unappealing feature of this theory.

The inverse decay rate for $p \to e^+\pi^0$ can be calculated in minimal SUSY $SU(5)$ to be [50, 51, 52]

$$\Gamma^{-1}(p \to e^+\pi^0) = (1.6 \times 10^{35}\ \text{yr}) \times \left(\frac{\alpha_H}{0.012\ \text{GeV}^3}\right)^{-2} \left(\frac{\alpha_G}{1/25}\right)^{-2} \left(\frac{A_R}{2.5}\right)^{-2} \left(\frac{M_X}{10^{16}\ \text{GeV}}\right)^{4} . \tag{13.2}$$

Here M_X is the mass of the X, Y gauge bosons that mediate proton decay, $\alpha_G = g_5^2/(4\pi) \simeq 1/25$ where g_5 is the unified gauge coupling, $\alpha_H \simeq 0.01\ \text{GeV}^3$ is the nuclear matrix element relevant for proton decay, and $A_R \simeq 2.5$ is the renormalization factor of the effective $d = 6$ proton decay operator. Naively one would expect M_X to be slightly below the unification scale $M_{\text{GUT}} \approx 2 \times 10^{16}$ GeV, since full unification is achieved at momentum scales above the masses of all split multiplets. Low energy gauge couplings do provide precise information on a particular combination of GUT scale masses:

$$(-2\alpha_3^{-1} - 3\alpha_2^{-1} + 3\alpha_Y^{-1})(M_Z) = \frac{1}{2\pi}\left\{36 \ln\left(\frac{M_X}{M_Z}\left(\frac{M_\Sigma}{M_X}\right)^{1/3}\right) + 8 \ln\left(\frac{M_{\text{SUSY}}}{M_Z}\right)\right\} . \tag{13.3}$$

Here the quantity on the LHS is experimentally measured with high precision. M_Σ on the RHS refers to the mass of a color octet Higgs field that is left-over from the GUT symmetry breaking. M_{SUSY} is the effective supersymmetry breaking mass scale, which is presumed to be known within specific schemes of SUSY breaking. It is the GUT mass of the color octet that is uncertain, which reflects in the proton lifetime estimate as well.

The mass of the other super-heavy particle of the theory, the color triplet superfield which mediates the decay $p \to \overline{\nu}K^+$, can also be related to low energy observables in analogy to Eq. (13.3). In general, agreement with the experimental value of $\alpha_3(M_Z) = 0.1184 \pm 0.0007$ demands the color triplet mass to be lower than $M_{\text{GUT}} \approx 2 \times 10^{16}$ GeV. This tends to lead to a rate of proton decay into $\bar{\nu}K^+$ which is in disagreement with observations [51], at least in the case where the superparticle masses are below about 3 TeV, so that they can be produced at the LHC.

It should be noted, however, that the Yukawa sector of minimal SUSY $SU(5)$ enters in a crucial way in the rate of proton decay into $\bar{\nu}K^+$. Minimal SUSY $SU(5)$ with renormalizable couplings leads to the relation $M_d = M_\ell^T$, relating the down quark and charged lepton mass matrices. Consequently, the asymptotic relations $m_b^0 = m_\tau^0,\ m_s^0 = m_\mu^0,\ m_d^0 = m_e^0$ follow for the masses of quarks and leptons at the GUT scale. Although the first of these relations agrees reasonably well with observations once it is extrapolated to low energies, the relations involving the two light family fermions are not in agreement with observations. Allowing for higher dimensional non-renormalizable operators can correct these wrong relations, however, they will also modify predictions for the decay rate $p \to \overline{\nu}K^+$ in a way that cannot be precisely pinned down. Thus the exclusion of the minimal renormalizable SUSY $SU(5)$ model based on the non-observation of the decay $p \to \overline{\nu}K^+$ should be taken with some reservation [52].

Various modifications of the Yukawa sector of minimal SUSY $SU(5)$ that correct the unacceptable fermion mass relations have been studied. One could introduce new Higgs fields belonging to a $45_H + \overline{45}_H$ representation [53], which would however, introduce large GUT scale threshold corrections. One could rely on higher dimensional operators to correct the fermion masses, which would also introduce a large number of parameters. An alternative possibility, which appears to be simple and predictive, is to add a vector-like pair of $\{5 + \overline{5}\}$ fermions [54]. The quarks and leptons from these multiplets can mix differently with the usual quarks and leptons, and thereby correct the bad mass relations $m_s^0 = m_\mu^0$ and $m_d^0 = m_e^0$. (Such mixings break $SU(5)$ symmetry through the vacuum expectation value of the 24_H Higgs field.) Optimizing these mixings so as to enhance the dominant $p \to \overline{\nu}K^+$ lifetime to saturate the present upper limit, approximate upper limits for the various partial lifetimes are found: $\tau(p \to \mu^+K^0) \sim 1 \cdot 10^{34}$ yrs, $\tau(p \to \mu^+\pi^0) \sim 2 \cdot 10^{34}$ yrs, and $\tau(p \to \overline{\nu}+\pi^0) \sim 7 \cdot 10^{33}$ yrs [54]. In obtaining these numbers, the SUSY particles have been assumed to have masses below 3 TeV, and the unification scale has been taken to be at least a factor of 50 below the

Planck scale, so that quantum gravity effects remain negligible. Here results of lattice calculations for the nuclear matrix element relevant for proton decay have been used [55]. Since the predicted rates are close to the present experimental limits, these realistic SUSY $SU(5)$ models can be tested by improving the current sensitivity for proton lifetime by a factor of ten.

13.2.2 $SO(10)$ Unification and Proton Decay

Models based on $SO(10)$ gauge symmetry are especially attractive since quarks, leptons, anti-quarks, and anti-leptons of a family are unified in a single **16**-dimensional spinor representation of the gauge group [39]. This explains the quantum numbers (electric charge, weak charge, color charge) of fermions, as depicted in Table 1. $SO(10)$ symmetry contains five independent internal spins, denoted as $+$ or $-$ signs (for spin–up and spin–down) in Table 1. Subject to the condition that the number of down spins must be even, there are 16 combinations for the spin orientations, each corresponding to one fermionic degree. The first three spins denote color charges, while the last two are weak charges. In addition to the three independent color spins (r, b, g), there is a fourth color (the fourth row), identified as lepton number [18]. The first and the third columns (and similarly the second and the fourth) are left–right conjugates. Thus $SO(10)$ contains quark–lepton symmetry as well as parity. A right–handed neutrino state (ν^c) is predicted because it is needed to complete the multiplet. Being a singlet of the Standard Model, it naturally acquires a superheavy Majorana mass and leads in a compelling manner to the generation of light neutrino masses via the seesaw mechanism. Hypercharge of each fermion follows from the formula $Y = \frac{1}{3}\Sigma(C) - \frac{1}{2}\Sigma(W)$, where $\Sigma(C)$ is the summation of color spins (first three entries) and $\Sigma(W)$ is the sum of weak spins (last two entries). This leads to quantization of hypercharge, and thus of electric charge. Such a simple organization of matter is remarkably beautiful and can be argued as a hint in favor of GUTs based on $SO(10)$.

$u_r : \{-++\ +-\}$	$d_r : \{-++\ -+\}$	$u_r^c : \{+--\ ++\}$	$d_r^c : \{+--\ --\}$
$u_b : \{+-+\ +-\}$	$d_b : \{+-+\ -+\}$	$u_b^c : \{-+-\ ++\}$	$d_b^c : \{-+-\ --\}$
$u_g : \{++-\ +-\}$	$d_g : \{++-\ -+\}$	$u_g^c : \{--+\ ++\}$	$d_g^c : \{--+\ --\}$
$\nu : \{---\ +-\}$	$e : \{---\ -+\}$	$\nu^c : \{+++\ ++\}$	$e^c : \{+++\ --\}$

Table 13-1. *Quantum numbers of quarks and leptons. The first three signs refer to color charge, and the last two to weak charge. To obtain hypercharge, use* $Y = \frac{1}{3}\Sigma(C) - \frac{1}{2}\Sigma(W)$.

As in the case of $SU(5)$, when embedded with low energy supersymmetry so that the mass of the Higgs boson is stabilized, the three gauge couplings of the Standard Model (SM) nearly unify at an energy scale of $M_X \approx 2 \cdot 10^{16}$ GeV in $SO(10)$ models. The light neutrino masses inferred from neutrino oscillation data ($m_{\nu_3} \sim 0.05$ eV) suggest the Majorana mass of the heaviest of the three ν^c's to be $M_{\nu^c} \sim 10^{14}$ GeV, which is close to M_X. In a class of $SO(10)$ models discussed further here, $M_{\nu^c} \sim M_X^2/M_{\rm Pl} \sim 10^{14}$ GeV quite naturally. The lepton number violating decays of ν^c can elegantly explain the observed baryon asymmetry of the universe via leptogenesis. Furthermore, the unified setup of quarks and leptons in $SO(10)$ serves as a powerful framework in realizing predictive schemes for the masses and mixings of all fermions, including the neutrinos, in association with flavor symmetries in many cases. All these features make SUSY $SO(10)$ models compelling candidates for the study of proton decay.

Even without supersymmetry, $SO(10)$ models are fully consistent with the unification of the three gauge couplings and the experimental limit on proton lifetime, unlike non–SUSY $SU(5)$. This is possible since $SO(10)$ can break to the SM via an intermediate symmetry such as $SU(4)_C \times SU(2)_L \times SU(2)_R$ [56]. Such models would predict that a proton would decay predominantly to $e^+\pi^0$ with a lifetime in the range $10^{33}-10^{36}$

yrs, depending on which intermediate gauge symmetry is realized [57]. If the intermediate symmetry is $SU(4)_C \times SU(2)_L \times SU(2)_R \times D$ with D being the discrete parity symmetry, then taking all the relevant threshold effects into account an upper limit on the lifetime $\tau(p \to e^+\pi^0) < 5 \times 10^{35}$ yrs has been derived in Ref. [58]. It has been shown in Ref. [59] that with the intermediate symmetry $SU(4)_C \times SU(2)_L \times SU(2)_R$ (without discrete parity), $SO(10)$ models can also explain the strong CP problem via the axion solution, although $\tau(p \to e^+\pi^0)$ in this case can exceed 5×10^{35} yrs.

In SUSY $SO(10)$ models, symmetry breaking can occur in two interesting ways. One type adopts a $\overline{\mathbf{126}}$ of Higgs, a tensor, which couples directly to the ν^c states and generates large Majorana masses for them. This class of models has the attractive feature that the R–parity of the Minimal Supersymmetry Standard Model (MSSM), which is so crucial for identifying the lightest SUSY particle as the dark matter candidate, is an automatic symmetry, which is part of $SO(10)$. In this category, a class of minimal $SO(10)$ models employing a single $\overline{\mathbf{126}}$ and a single $\mathbf{10}$ of Higgs bosons that couple to the fermions has been developed [60]. Owing to their minimality, these models are quite predictive as regards the neutrino mass spectrum and oscillation angles. Small quark mixing angles and large neutrino oscillation angles emerge simultaneously in these models, despite their parity at the fundamental level. The neutrino oscillation angle θ_{13} is predicted to be large in these models. In fact, this mixing angle was predicted to be $\sin^2 2\theta_{13} \simeq 0.09$, well before it was measured to have this central value [61]. Proton decay studies of these models [62] show that at least some of the modes among $p \to \overline{\nu}\pi^+$, $n \to \overline{\nu}\pi^0$, $p \to \mu^+\pi^0$ and $p \to \mu^+K^0$ have inverse decay rates of order 10^{34} yrs, while that for $p \to e^+\pi^0$ is of order 10^{35} yrs. These upper limits are obtained by saturating $\Gamma(p \to \overline{\nu}K^+)$ with the experimental limit.

The second type of SUSY $SO(10)$ model adopts a set of low-dimensional Higgs fields for symmetry breaking [63]–[69]. This includes spinors $\mathbf{16}+\overline{\mathbf{16}}$, vectors $\mathbf{10}$ and an adjoint $\mathbf{45}$ which acquires a vacuum expectation value along the $B-L$ direction of the form $\langle A \rangle = \mathrm{i}\sigma_2 \otimes \mathrm{Diag}\,(a,\ a,\ a,\ 0,\ 0)$. This has quite an interesting effect [63], [64], since it would leave a pair of Higgs doublets from the $\mathbf{10}$ naturally light, while giving superheavy mass to the color triplets – a feature that is necessary to avoid rapid proton decay – when the $\mathbf{45}$ couples to the vector $\mathbf{10}$–plets. Doublet–triplet splitting is achieved in these models without the need for fine-tuning. These models predict that the heaviest of the light neutrinos has a mass that is naturally of order one tenth of an eV, consistent with atmospheric neutrino oscillation data. This setup also allows for a predictive system for fermion masses and mixings, in combination with a flavor symmetry. Models that appear rather different in the fermion mass matrix sector result in very similar predictions for $p \to \overline{\nu}K^+$ inverse decay rate, which has been found to be typically shorter than a few times 10^{34} yrs [63]–[69].

Recent work in the same class of SUSY $SO(10)$ models which adopt small Higgs representations has shown that there is an interesting correlation between the inverse decay rates for the $p \to \overline{\nu}K^+$ and $p \to e^+\pi^0$ modes. The amplitude for the former scales inversely as the three-halves power of that for the latter, with only a mild dependence on the SUSY spectrum in the constant of proportionality [69]. This intriguing correlation leads to the most interesting result that the experimental lower limit of the lifetime for $p \to \overline{\nu}K^+$ decay provides a theoretical upper limit on the lifetime for $p \to e^+\pi^0$ decay, and vice versa. An updated version of the work of [69] has been carried out [70] by incorporating the latest LHC limits on the masses of the SUSY particles and using a Higgs mass of 126 GeV, while preserving a reasonable degree of SUSY naturalness. As a typical case, one finds:

$$\begin{aligned} \tau(p \to e^+\pi^0) &\leq 6.8 \times 10^{34}\ \text{yrs}\,, \\ \tau(p \to \overline{\nu}K^+) &\leq \left(7 \times 10^{34}\ \text{yrs}\right) \cdot \left(\frac{\hat{m}_{\tilde{q}}}{2.4\ \text{TeV}}\right)^4 \cdot \left(\frac{550\ \text{GeV}}{m_{\tilde{W}}}\right)^2 \cdot \left(\frac{7}{\tan\beta}\right)^2 . \end{aligned} \tag{13.4}$$

Here $\hat{m}_{\tilde{q}}$ stands for a weighted effective mass of the squarks of the three families. Thus we see that these predictions are accessible to future experiments, with an improvement in current sensitivity by about a factor of 10.

It has been argued that well-motivated supersymmetric GUTs generically predict proton decay rates that can be probed by next-generation experiments. One could conceive, however, variations of these predictions by either some cancellation of contributions from different $\mathcal{B}$- and $\mathcal{L}$-violating dimension-five operators [71], by suppression of Higgsino couplings with matter, by judicious choice of the flavor structure [72], or by the largeness of the scalar masses (see, for example, Ref. [73]). For further studies see Ref. [74]–[78], and for a connection between the inflation mechanism and the proton decay rate, see, for example, Ref. [79].

Let us stress in closing that an important prediction of the simple $SU(5)$ and $SO(10)$ GUTs is that proton decay modes obey the selection rule $\Delta(\mathcal{B}-\mathcal{L})=0$ and are mediated by effective operators with dim=6. A general effective operator analysis of baryon number violation reveals two conclusions. One is that $\Delta\mathcal{B}\neq 0$ operators with dim=7 always predict that $|\Delta(\mathcal{B}-\mathcal{L})|=2$, which leads to decays such as $n\to e^-+\pi^+$. These $d=7$ operators that lead to the selection rule $|\Delta(\mathcal{B}-\mathcal{L})|=2$ have been shown to arise in $SO(10)$ GUTs [80], and may lead to observable nucleon decay rates in the non–supersymmetric models with an intermediate scale associated with a symmetry or new particles.

13.2.3 Proton Decay in Extra Dimensional GUTs

In higher dimensions it is possible to solve the doublet–triplet splitting problem in an elegant way via boundary conditions in the extra dimensions [81]. In such a setup it is possible to maintain the success of SUSY GUTs as regards the unification of gauge couplings [82],[83].

String theories that manifest the nice features of 4D SUSY GUTs have been constructed with a discrete Z_4^R symmetry. This symmetry prevents dimension 3, 4 and 5 lepton and baryon number violating operators, which are potentially dangerous, to all orders in perturbation theory. The μ-term (the Higgsino mass term in the MSSM) also vanishes perturbatively. However non-perturbative effects will generate a μ-term of order the SUSY breaking scale, as desired. On the other hand, the low energy theory is guaranteed to be invariant under matter parity. Thus the lightest SUSY particle is stable and is an excellent dark matter candidate.

Nucleon decay in theories with a Z_4^R symmetry [84],[85] is dominated by dimension 6 operators which lead to the classic decay modes, $p\to e^+\pi^0, \bar{\nu}\pi^+$ and $n\to\bar{\nu}\pi^0, e^+\pi^-$. The lifetime for these modes is of order $\tau\sim\frac{M_C^4}{\alpha_G^2 m_p^5}$ where M_C is the compactification scale of the extra dimension. This scale is typically less than the 4D GUT scale, *i.e.*, $M_C\leq M_{\rm GUT}\approx 2\times 10^{16}$ GeV. Thus the rate for nucleon decay in these modes is typically also within the reach of the next generation of experiments. Moreover, due to the absence of $p\to\overline{\nu}K^+$ decay mode, the observation of proton decay only in the $e^+\pi^0$ mode may allow one to distinguish minimal four-dimensional unification models from extra-dimensional ones.

13.2.4 Induced Nucleon Decay and Asymmetric Dark Matter

In this subsection we summarize a novel way for nucleon decay, which is motivated by a desire to understand the dark matter fraction in the Universe, in relation to the baryon fraction. The energy density of dark matter (DM) is about five times larger than that of visible baryonic matter (protons and neutrons). Yet, given that DM has very different properties from baryons, one may wonder why these two types of matter have fairly similar shares of the cosmic energy budget. One explanation is that DM and baryons share a common origin. The baryon density today originated from an asymmetry between baryons and antibaryons; when they annihilated, only baryons were left–over. Similarly, DM may have a primordial asymmetry comparable to the baryon asymmetry in the Universe, so that when DM particles and antiparticles annihilated during

freeze-out, only the residual asymmetric component remained [86]. Typically, this implies that the DM mass is below the weak scale.

If DM and baryons are related, it has been proposed [87] that unusual DM signatures involving baryon number violation can arise: DM in the local halo can annihilate nucleons, producing energetic mesons that can be observed in terrestrial experiments. This process, termed *induced nucleon decay* (IND), mimics traditional nucleon decay since the DM states are unobserved. However, the kinematics of the daughter mesons is different for IND, requiring different analyses compared to existing searches [88]. In a minimal model, DM is composed of a pair of stable states: a scalar-fermion pair denoted by Φ, Ψ [87, 88] (e.g., these states may be SUSY partners [89]). The DM operator $\Phi\Psi$ may couple to a neutral combination of light quarks such as *udd* or *uds*, giving rise to effective interactions between baryons, mesons, and DM. These interactions lead to inelastic scattering $\Phi\, N \to \bar{\Psi}\, \Pi$ or $\Psi\, N \to \Phi^*\, \Pi$, where N is the nucleon and Π is a meson (pion, kaon, etc.). DM *particles* are transmuted into *antiparticles* ($\bar{\Psi}, \Phi^*$) by annihilating visible baryons through inelastic scattering. Since both the initial and final state dark particles are not observed, these processes resemble nucleon decay into neutrino final states, $N \to \Pi\, \nu$.

For typical values of parameters, the momentum p_Π of the final state meson in an IND scattering is $\sim 0.6 - 1.4$ GeV. This provides a kinematic discriminant between IND and standard nucleon decay (SND), which typically has $p_\Pi \lesssim 0.5$ GeV. The IND scattering rate depends on the hadronic matrix element of the three-quark operator between a nucleon and a meson. To get an order-of-magnitude estimate for the effective lifetime of a nucleon within the local DM halo, Refs. [87, 88] used chiral perturbation theory and found

$$\tau_N^{\rm eff} \approx 10^{32}\ {\rm yr} \times \left(\frac{\Lambda_{\rm IND}}{1\ {\rm TeV}}\right)^6 \left(\frac{0.3\ {\rm GeV/cm^3}}{\rho_{\rm DM}}\right), \tag{13.5}$$

where $\Lambda_{\rm IND}$ is the mass scale of the quark-DM nonrenormalizable coupling and $\rho_{\rm DM}$ is the local energy density of DM. It should be cautioned that chiral perturbation theory is valid for $p_\Pi \ll 1$ GeV and more precise estimates require fully non-perturbative lattice calculations [90]. Given that new TeV-scale physics may play a role in electroweak symmetry breaking, one could reasonably assume that $\Lambda_{\rm IND} \gtrsim 1$ TeV. It is quite interesting that the estimate of Eq. (13.5) for $\tau_N^{\rm eff}$ is close to the current and future limits on nucleon lifetimes τ_N from SND experiments.

IND searches have a natural complementarity with LHC searches for DM. The operator that connects light quarks (q) and DM can mediate monojet processes of the type $q\, q \to \bar{q} + E_T^{\rm miss}$, where $E_T^{\rm miss}$ is missing transverse energy from DM escaping the detector. The estimates in Ref. [88] suggest that the LHC at $\sqrt{s} = 14$ TeV and with $\mathcal{O}(100\ {\rm fb}^{-1})$ of integrated luminosity can be sensitive to $\Lambda_{\rm IND} \sim 1 - 4$ TeV, albeit with some model dependence resulting from underlying ultraviolet physics. Hence, given the estimate of Eq. (13.5), one would typically expect a direct correlation between observable signals of IND at nucleon decay experiments and at the LHC.

13.2.5 Gauging Baryon Number

Grand Unified Theories, while elegant, must be realized at a very high energy scale of order 10^{16} GeV, well beyond the reach of foreseeable accelerators for direct detection of new particles. It is possible to understand the approximate conservation of baryon number by making $\mathcal{B}$ a *local* symmetry [91, 92]. This would require additional fermions for anomaly cancelation, since $\mathcal{B}$ is an anomalous symmetry with respect to the weak interactions. In such theories with gauged $\mathcal{B}$, spontaneous symmetry breaking may occur at relatively low energies, which may be accessible to colliders. Model building with the inclusion of new fermions in order to gauge $\mathcal{B}$ has been studied in great detail in Refs. [93, 94]. In these papers it has been shown that simple

extensions of the SM with a local $\mathcal{B}$ symmetry broken at the TeV scale are fully consistent with experimental constraints, including cosmology. This class of theories could open a new path to probing the origin of approximate $\mathcal{B}$ conservation.

13.3 Nucleon Decay Experiments: Past, Present and Future

When Grand Unified Theories were formulated in the mid-1970's, they predicted lifetimes of the nucleon as short as 10^{29} years, which put experimental detection within range of kiloton scale detectors. First generation experiments were quickly proposed and mounted: IMB and Soudan in the United States, Kamiokande in Japan, NUSEX and Frejus in Europe. None of these experiments found a significant signal, and notably, IMB and Kamiokande excluded the minimal $SU(5)$ prediction for the decay $p \to e^+\pi^0$. The limits from these experiments populate roughly 70 exclusive decay modes tabulated by the Particle Data Group [95].

The second generation is singularly comprised of the Super-Kamiokande experiment, which began in 1996 and is ongoing. Super-Kamiokande also has never yet found a significant nucleon decay signal. The experiment has extended the lifetime limits for numerous modes by more than an order of magnitude over the first generation experiments. As of early 2013, the Super-Kamiokande collaboration have recorded 260 kiloton·years of exposure with partial lifetime limits in the range 10^{33} to 10^{34} years in many cases. The results from Super-Kamiokande provide both a baseline for comparison and challenge to the next generation experiments. The next subsection reviews the results from Super-Kamiokande.

13.3.1 Super-Kamiokande Searches for Nucleon Decay

The Super-Kamiokande water Cherenkov experiment dominates the current limits set on the lifetime of the proton and bound neutron. The 22,500-ton fiducial mass of the detector has 7.5×10^{33} protons and 6.0×10^{33} neutrons. Fully contained atmospheric neutrino interactions in the GeV range constitute the background. The experiment has been collecting data since 1996 with four distinct data-taking periods called SK-I, -II, -III, and -IV. During the SK-I, -III, and -IV periods, ∼11,000 inward-facing 20-inch photomultiplier tubes (PMTs) were distributed evenly on the entire inner detector (ID) surface to provide 40% photocathode coverage. An accident that destroyed roughly half of the PMTs in the inner detector led to the the SK-II period, where the remaining functional PMTs were redistributed evenly across the ID surface with approximately 20% photocathode coverage. This SK-II period of reduced coverage is notable for future generation water Cherenkov detectors because the Super-K nucleon decay and atmospheric neutrino analyses show that the reduction in photocathode coverage does not have a large adverse effect on nucleon decay detection efficiency or background rejection. Photodetection drives the cost of large water Cherenkov detectors, and containing this cost is of great importance. The SK-IV period introduced new electronics, and incremental gains in detection efficiency or background rejection are seen in some analyses.

There are several methods of searching for nucleon decay. The most straightforward method is to define a set of selection criteria that maximize the signal detection efficiency and minimize the background. The $p \to e^+\pi^0$ mode is a good example of this technique. The proton decay signal is simulated using a Monte Carlo program that includes effects due to Fermi motion, nuclear binding potential, intranuclear reactions, and correlated nucleon effects (all of which are absent for the free proton that is the hydrogen nucleus). Deleterious nuclear effects are largely responsible for the overall signal efficiency of roughly 40%. The background is estimated by a simulated 500 year exposure of atmospheric neutrinos using the detailed model that is standard for Super-K, one that takes into account the atmospheric neutrino flux, neutrino-

nucleus cross sections, and interactions within the nucleus. The signal efficiency and background rates are summarized in Table 13-2. The systematic uncertainty in the efficiency is estimated to be 19% and the systematic uncertainty in the background rate is estimated to be 44%, independent of SK period. The background rate has been independently checked using GeV-scale muon neutrino data in the 1-kiloton water Cherenkov detector that served as a near detector in the K2K long-baseline neutrino oscillation experiment [96]. The preliminary Super-K result for $p \to e^+\pi^0$, as of 2013, is detection of zero candidate events and a 90% C.L. limit on the partial lifetime of 1.4×10^{34} years [97].

Table 13-2. *Signal efficiency and background rates for the $p \to e^+\pi^0$ analyses by Super-Kamiokande. Uncertainties listed are statistical, due to the Monte Carlo event sample. These are preliminary numbers based on improved and updated analyses from those published in 2011 [98].*

	data livetime	$p \to e^+\pi^0$ signal efficiency	atmos. ν estimated bkg.	atmos. ν bkg. rate (evts/Mt/y)
SK-I	91.7 kt y	$39.2 \pm 0.7\%$	0.27 evts.	2.9 ± 0.6
SK-II	49.2 kt y	$38.5 \pm 0.7\%$	0.15 evts.	3.0 ± 0.5
SK-III	31.9 kt y	$40.1 \pm 0.7\%$	0.07 evts.	2.3 ± 0.6
SK-IV	87.3 kt y	$39.5 \pm 0.7\%$	0.22 evts.	2.5 ± 0.6
K2K				$1.63^{+0.42}_{-0.33}(\text{stat})^{+0.45}_{-0.51}(\text{sys})$

As can be seen in Fig. 13.3.1, the signal region is defined by a box indicating the expected ranges of total reconstructed momentum and invariant proton mass. The background events that pass all other selection cuts (atmospheric neutrino interactions) do not typically fall into the range of momentum and invariant mass that one expects for proton decay events, making this a low-background search mode. As long as background rates are kept small (no more than a few events, preferably less than one), future large water Cherenkov detectors will extend these limits by a factor of the increase in detector mass times running time. Also, for searches with background estimates substantially lower than 1 event, discovery of proton decay by a single clean event remains possible.

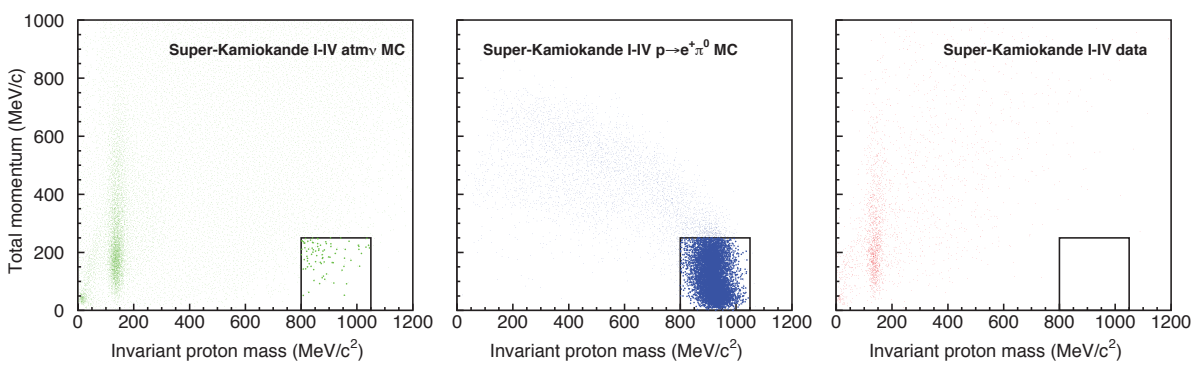

Figure 13-3. *The combined SK-I+II+III+IV analysis of $p \to e^+\pi 0$.*

.

A second technique is used for some decay modes in which a low background cannot be achieved. For these modes, a "bump search" is done. Example of this are $n \to \nu\pi^0$ and $p \to \nu\pi^+$, where one looks for a momentum peak from mono-energetic single pions on top of a background consisting mostly of atmospheric neutrino events with a single π^0 or non-showering ring[99]. For this type of search, understanding the shape of the background event spectrum is critical. Because these searches are inherently background limited, future large water Cherenkov detectors will not greatly extend the sensitivity.

The search for the SUSY GUT favored $p \to \overline{\nu}K^+$ mode is basically a search for K^+ decay at rest, as the kaon from proton decay is below the Cherenkov threshold. For the kaon decay to $\pi^+\pi^0$ (branching ratio of 21%), selection criteria are used as described above. For the largest branching ratio, $K^+ \to \mu^+\nu_\mu$ (64%), Super-K uses a combination of the bump search technique plus a low-background cut-based analysis that tags events by a low energy photon from the de-excitation of the excited nucleus that is left after the decay of a proton in ^{16}O. Using a combination of these techniques allows the measurement to push the limit on the proton decay lifetime further than using any of the individual methods. The combined efficiency and background rates for the low-background selections of $\pi^+\pi^0$ and nuclear-γ tag are shown in Table 13-3. The weaker performance of SK-II with 20% photocoverage is now evident, due to decreased ability to separate 6 MeV nuclear gamma rays from background. Improved performance due to upgraded electronics in SK-4 is also evident, mainly due to increased efficiency for identifying Michel electrons.

Table 13-3. *Signal efficiency and background rates for the $p \to \nu K^+$ analyses by Super-Kamiokande. Uncertainties listed are statistical, due to the Monte Carlo event sample. These are preliminary numbers based on improved and updated analyses from those reported as late as 2012. The efficiencies and background rates are for the combination of the relatively low-background techniques: $K^+ \to \pi^+\pi^0$ plus $K^+ \to \nu_\mu\mu^+$ with nuclear-γ tag.*

	data livetime	$p \to \nu K^+$ signal efficiency	atmos. ν estimated bkg.	atmos. ν bkg. rate (evts/Mt/y)
SK-I	91.7 kt y	$15.7 \pm 0.2\%$	0.3 evts.	2.8 ± 0.4
SK-II	49.2 kt y	$13.0 \pm 0.2\%$	0.3 evts.	6.2 ± 0.8
SK-III	31.9 kt y	$15.6 \pm 0.2\%$	0.1 evts.	3.1 ± 0.5
SK-IV	87.3 kt y	$19.1 \pm 0.2\%$	0.3 evts.	3.5 ± 0.4

No signs of nucleon decay have been seen yet in any Super-K analysis of any nucleon decay mode. The 90% C.L. lifetime limits of Super-K nucleon decay searches to antilepton plus meson are summarized in Fig 13-4, compared with measurements from past experiments. These are two-body decay modes that conserve $(B - L)$. As mentioned previously, although many GUTs automatically predict one or more of these modes with varying branching ratios, it is important to also consider three-body decay modes and alternative origins of baryon number violation that conserve $(B + L)$[1] or violate only B (e.g. dinucleon decay). Studies along these lines are an active area of inquiry within the Super-Kamiokande collaboration and a handful of first results, all negative so far, are presented in talks, theses, or are being prepared for publication.

[1] Decay modes with a final state neutrino, always unobserved, may be interpreted as conserving $(B - L)$ or $(B + L)$

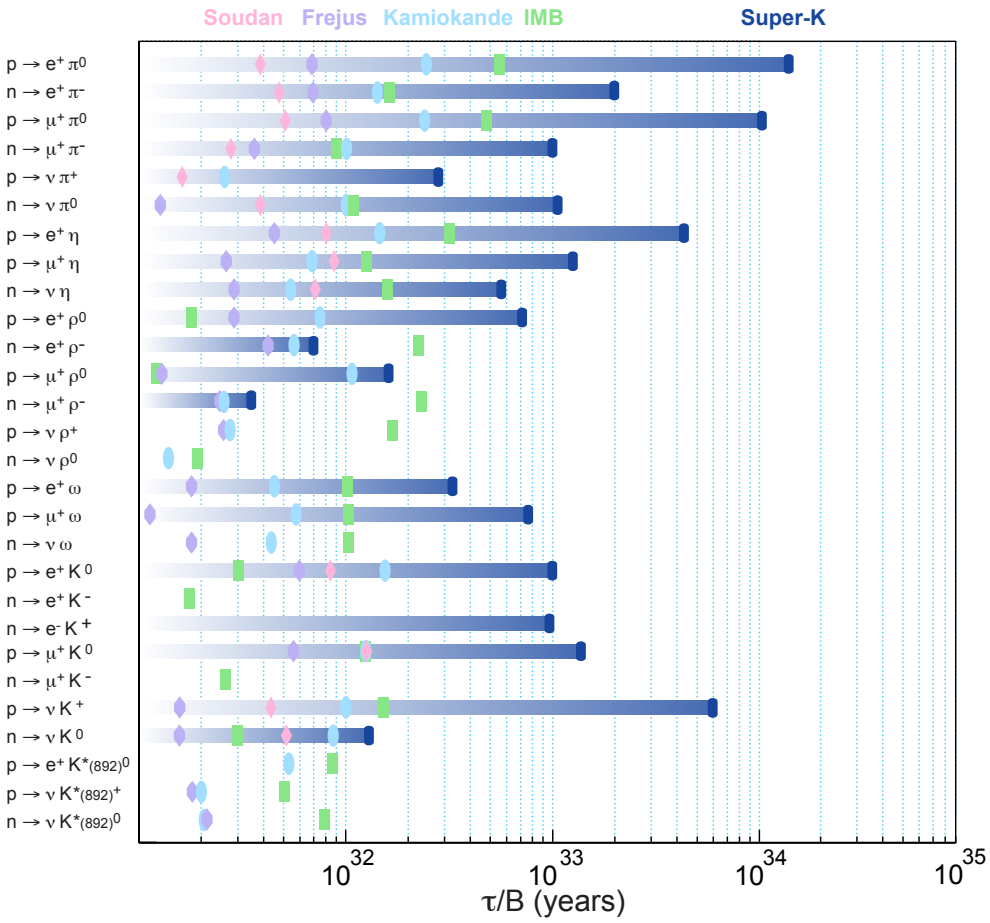

Figure 13-4. *Summary of lifetime limits for proton or bound neutron decay into antilepton plus meson; the complete set of possible two-body decay modes that conserve $B - L$ is listed. Experimental searches were conducted by Super-K (dark blue gradient band with marker) and previous experiments: Soudan (pink diamonds), Frejus (purple hexagons), Kamiokande (light blue ovals), and IMB (light green rectangles).*

13.3.2 Proposed Proton Decay Search Experiments

There are a variety of proposals to continue the search for nucleon decay with a new generation of experiments. Some of these proposals are inactive or discontinued, while others are being actively discussed in various parts of the world. The proposed detectors can be categorized broadly in three distinctive technologies: water Cherenkov detectors, liquid argon TPCs and scintillator detectors. Table 13-4 shows a summary of the proposed projects categorized by technology and region. Not included are some large detectors that may be able to contribute but that have not developed the case for proton decay (for example multi-kiloton reactor experiments using liquid scintillator).

Table 13-4. *Next generation nucleon decay detector proposals. Inactive efforts are marked with an asterisk. Speculative future projects that are less fully-developed and that may be considered for a future generation are marked with a dagger.*

Name	Technology	Mass	Location	Reference
Hyper-K	WC	560 kt	Japan	[100]
LBNE	LArTPC	10-70 kt	U.S.	[101]
LENA	Scintillator	50 kton	Europe	[102]
GLACIER	LArTPC	20-100 kt	Europe	[103]
MEMPHYS	WC	500 kton	Europe	[104]
WbLSc	Scintillator	23 kton	Japan	[105]
LBNE-WC	WC	100-200 kton	U.S.	*[101]
UNO	WC	440 kton	U.S.	*[106]
LANDD	LArTPC	$n\times$ 5 kton	U.S.	*[107]
MICA	WC (ice)	multi-Mton	South Pole	† [108]
TITAND	WC	multi-Mton	ocean	† [109]

In the following sections, the search for nucleon decay in each of the three categories: water Cherenkov, liquid argon TPC (LArTPC), and scintillator are described, with an emphasis on the leading candidate experiment for each technology.

13.3.3 Water Cherenkov

A next-generation underground water Cherenkov detector, Hyper-Kamiokande (Hyper-K), is proposed for location in the Kamioka mine in Japan. It will serve as the far detector of a long baseline neutrino oscillation experiment using the off-axis J-PARC neutrino beam, and as a detector capable of observing nucleon decays, atmospheric neutrinos, and neutrinos from astronomical origin. The baseline design of Hyper-K is based on the highly successful Super-K experiment, taking full advantage of well-proven methods and technology. The fiducial mass of the detector is planned for 0.56 million metric tons, which is about 25 times larger than that of Super-K. The details of the proposed experiment can be found in a published Letter of Intent [100]. The Hyper-Kamiokande group has had several open organizational meetings over the past two years.

The sensitivity of Hyper-K for nucleon decays has been studied based on scaling of the the Super-Kamiokande analysis. The numbers for signal efficiency and background rate from atmospheric neutrinos are assumed to be identical to those used in the Super-K analyses reported in Section 13.3.1. Due to the very large mass and good energy and Cherenkov ring reconstruction in the GeV range, water Cherenkov is the best detector technology for signatures such as $e^+\pi$ and $\mu^+\pi^0$. As was shown with Super-K analyses, the efficiency and background rates are nearly unchanged if the photon coverage is 20% instead of 40%. It is likely that the effective photon coverage for Hyper-K will between those values. The planned number of PMTs, 99000, corresponds to 20% coverage; however recent PMT manufacturing by Hamamatsu offers higher quantum efficiency than previous generation PMTs such as those used in Super-K. It is safe to assume an overall signal efficiency of 40%, where the inefficiency is dominated by nuclear interaction of the pion. For comparison, the detection efficiency for decay of a free proton in H_2O is 87%. The background rate is well-established as discussed in the previous section, and one can conservatively assume 2 events per Mton-years. Based on these numbers, the 90% C.L. sensitivity of Hyper-K for a 10-year exposure is greater than 10^{35} years, as shown in Fig. 13-5.

Assuming the same analysis techniques employed by Super-Kamiokande, one can estimate the sensitivity of Hyper-Kamiokande. Most sensitivity comes from the two relatively background-free techniques: $K^+ \to \pi^+\pi^0$ and $K \to \mu^+\nu$ with nuclear-γ tag. Based on the background rate in Table 13-3, a 10-year exposure would have an expected background between 20 and 35 events. If the detected number of events are equal to the background rate, the 90% C.L. limit would be roughly 3×10^{34} years. This estimation assumes no reoptimization of the analysis (tighter cuts) to accomodate the higher background rate has been performed. Fig. 13-5 shows the 90% CL sensitivity curve for the $p \to \overline{\nu}K^+$ mode as a function of the detector exposure.

13.3.4 Liquid Argon TPC

The uniqueness of proton decay signatures in the LArTPC and the potential for fully reconstructing the final state has long been recognized as a strength for this technology. The LArTPC can reconstruct all final state charged particles including an accurate assessment of particle type, distinguishing muons from pions from kaons from protons. Electromagnetic showers are readily measured with a significant ability to distinguish those that originate from photons from π^0 decay from those that originate from charged-current electron neutrino interactions. Kiloton-per-kiloton, LAr TPC technology will outperform water cherenkov in both detection efficiency and atmospheric neutrino background rejection for most nucleon decay modes, although intranuclear effects are smaller for oxygen and non-existent for hydrogen.

Taking mass and cost into account, water Cherenkov technology is optimum for the $p \to e^+\pi^0$ final state topology, where the signal efficiency is roughly 40% and the background rate is 2 events per megaton-year. The estimate [110] for a LAr TPC is 45% efficiency and a background rate of 1 event per megaton year, not enough of an improvement to overcome the penalty of lower mass.

On the other hand, for the $p \to \nu K^+$ channel, the Super-K analysis yields a signal efficiency of roughly 19% for a background rate of 4 events per megaton year. This is the best mode for a LArTPC, where the K^+ track is reconstructed and identified as a charged kaon. The charged kaon, with a momentum of 340 MeV/c (neglecting nuclear effects), has a range of 14 cm in LAr, so ionization energy loss measurements are expected to give high particle identification efficiency. The decay products of the kaon are also identified with high efficiency, for all kaon decay branches. Fig. 13-6 shows an example event display of an isolated charged kaon found in surface cosmic ray test run of the ICARUS detector. The relative ionization of the kaon and muon are readily evident, including the Bragg peak as the charged particle comes to rest.

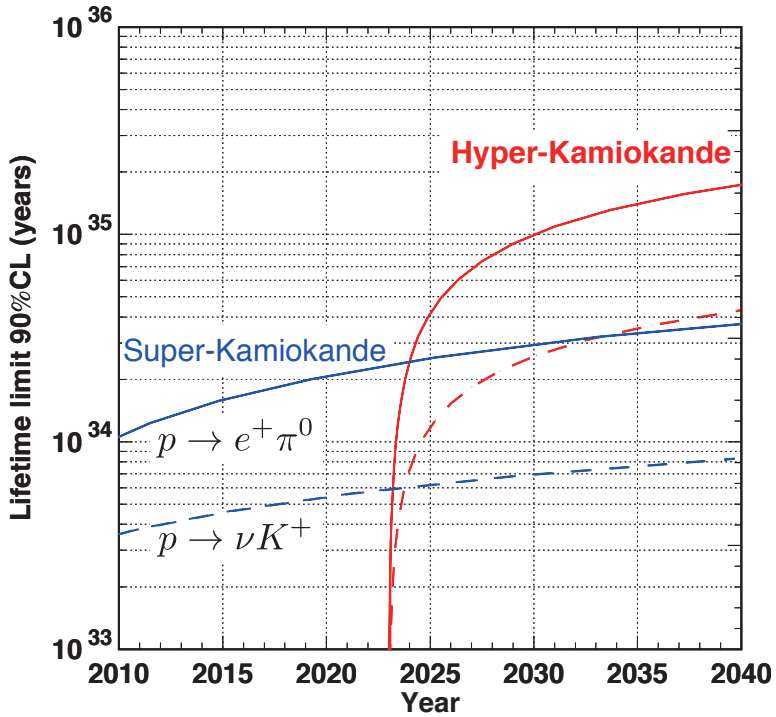

Figure 13-5. *Sensitivities of the Hyper-Kamiokande proton decay search as a function of detector exposure, at the 90% C.L. The blue curves on the left side shows the expected sensitivity for continued running of Super-K; the red curves on the right show the sensitivity for Hyper-Kamiokande. The upper solid curves are for $p \to e^+\pi^0$, for both experiments; the lower solid curve are for $p \to \nu K^+$.*

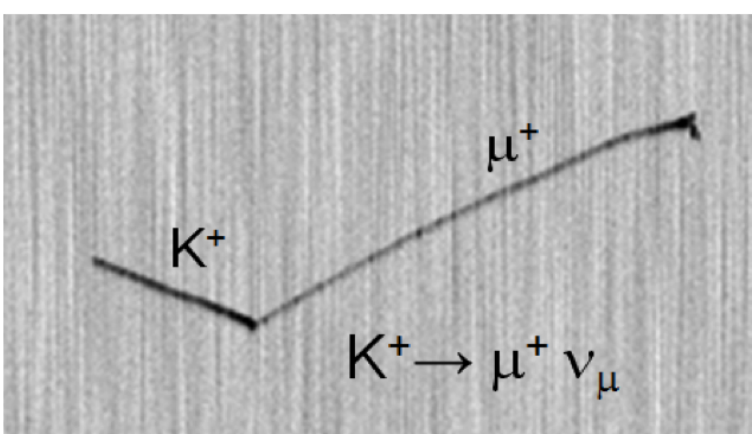

Figure 13-6. *Single event display for an isolated charged kaon in the ICARUS T600 detector. In this event, the kaon is observed as a heavily ionizing track that stops and decays to $\mu\nu$, producing a muon track that also stops and decays with a visible Michel electron.*

The total efficiency for the νK^+ mode is estimated to be as high as 96.8% with a background rate of 1 event per megaton year. Based on these numbers and a ten year exposure, the 34 kton LBNE detector and 560 kton Hyper-Kamiokande have comparable sensitivity (at 90% CL), but the LArTPC would have an estimated background of 0.3 events compared to tens of events for Hyper-K. Experimental searches for rare events in the presence of significant backgrounds are notoriously more problematic than background-free searches. A 10-year exposure of the 34-kton LBNE LArTPC detector would set a partial lifetime limit of roughly 3×10^{34} years, which is roughly the same as the sensitivity of Hyper-K, despite 20 times fewer proton-years. Figure 13-7 shows the expected limit on the proton lifetime as a function of time in LBNE for $p \to \nu K^+$.

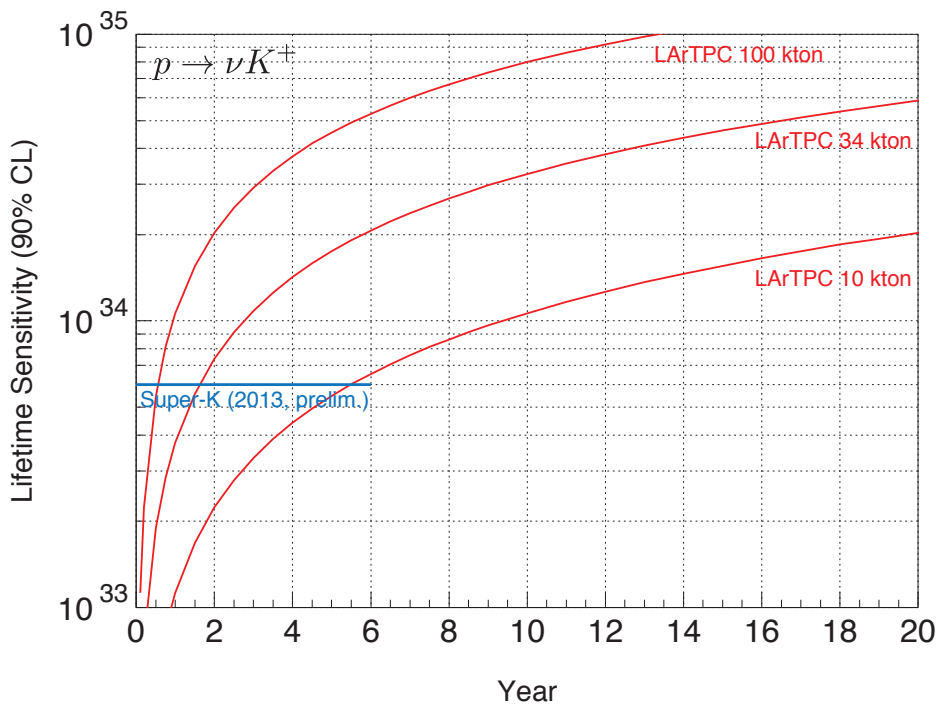

Figure 13-7. *Proton decay lifetime limit for $p \to K^+\bar{\nu}$ as a function of time for various masses of a LArTPC, assumed to be sufficiently deep that a low background rate is achieved. For comparison, the 2013 preliminary result from Super-K for 11.6 live years is drawn. The projected limits are at 90% C.L., calculated for a Poisson process including background assuming that the detected events equal the expected background.*

The LBNE LAr TPC has a chance to make up for lower detector mass when compared to Hyper-Kamiokande for nucleon decay modes where a water Cherenkov detector has relatively low efficiency or is susceptible to higher background rates. Because the LAr TPC can reconstruct protons that would otherwise be below Cherenkov threshold, it can reject many CC and NC background topologies by vetoing on the presence of a recoil proton. Because the LAr TPC has high spatial resolution, it does well for event topologies with displaced vertices (such as $p \to \mu^+ K^0$, a mode preferred in some SUSY GUTs over νK^+. For modes with no electron in the final state, the same displaced vertex performance we rely on for long-baseline neutrino oscillation allows the rejection of charged current ν_e interactions. In general, the above criteria favor nucleon decay modes with a kaon, charged or neutral, in the final state. Conversely, the efficiency for decay modes

to a lepton plus light meson will be limited by intranuclear reactions that are, if anything, worse than the case of ^{16}O in a water cherenkov detector.

An extensive survey of nucleon decay efficiency and background rates has been published [110]. The table below lists selected modes where a LAr TPC has a significant performance advantage (per kiloton) over the water Cherenkov technique.

Table 13-5. *Nucleon decay modes for which a LArTPC has an advantage in signal efficiency and background rejection over a water Cherenkov detector.*

decay mode	WC Efficiency	WC Bkg. Rate	LArTPC Efficiency	LArTPC Bkg. Rate
$p \to \nu K^+$	19%	4 /Mt/y	97%	1 /Mt/y
$p \to \mu^+ K^0$	10%	8 /Mt/y	47%	<2 /Mt/y
$p \to \mu^- \pi^+ K^+$			97%	<2 /Mt/y
$p \to e^- K^+$	10%	3 /Mt/y	96%	<2 /Mt/y
$p \to e^+ \pi^-$	19%	2 /Mt/y	44%	0.8 /Mt/y

13.3.5 Liquid Scintillator

There remains a final experimental technique that may be used to search for the favored proton decay mode $p \to \nu K^+$. In a water Cherenkov detector, the kaon is below Cherenkov threshold and produces no Cherenkov light. In a scintillator detector, the kaon will produce scintillation light with a yield of 100 or more photons per MeV deposited. A fast scintillator and photomultipliers should be able to resolve the sequential decay of the kaon ($tau \sim 12$ ns) followed by the decay of the muon ($\tau \sim 2.2\mu$s). The superior energy resolution resulting from more collected photons will assist in signal identification. Large (10+ kton scale) scintillator detectors are envisioned for neutrino physics, astrophysics, and recently, reactor neutrino oscillation (e.g Daya Bay 2). Except for this particular decay mode, the proposed liquid scintillator detectors do not have the mass or efficiency to compete with Hyper-Kamiokande or a comparable size LArTPC for any other modes. However, the proposed 50-kton LENA detector would be competitive with Hyper-Kamiokande or a 34 kton LArTPC at LBNE for $p \to \nu K^+$.

LENA[102] (Low Energy Neutrino Astronomy) is an unsegmented liquid-scintillator detector of 50-kt target mass proposed within the European LAGUNO-LBNO design study. While the emphasis of the LENA physics program is on low-energy neutrinos and anti-neutrinos (E<100 MeV), the search for proton decay into kaons and antineutrinos was one of the first items considered to play an integral part in the LENA concept, since the visibility of the kaon's energy deposition in the scintillator substantially increases the detection efficiency in comparison to water Cherenkov detectors. Monte Carlo simulations show that analysis cuts can be defined which retains a detection efficiency of $\sim 65\%$ for the proton decay signal. The search in LENA is expected to be background-free for about 10 years, allowing a lifetime limit of $\tau > 4 \times 10^{34}$ yrs (90% CL) if no event is observed.

Whereas LENA requires a substantial investment in a new cavern and detector, it is possible to envision a liquid scintillator upgrade to Super-Kamiokande. A white paper[105] suggests a water-based scintillator targeting a future upgrade for the 22.5 kton Super-Kamiokande. A ten-year exposure could reach a 90%

C.L. sensitivity on the partial lifetime of $p \to \nu K^+$ of 2×10^{34} years given favorable signal efficiency and background rejection.

13.4 Neutron-Antineutron Oscillations

In this section and the next we turn to the $|\Delta\mathcal{B}| = 2$ process, neutron–antineutron oscillations. The physics motivations are outlined here, followed by the experimental techniques focussing on the potential improvement over past free neutron beam experiment by as much as four orders of magnitude in transition probability will be addressed.

13.4.1 Physics Motivation for $n - \bar{n}$ Searches

Historically, the idea that neutron may be its own antiparticle was first conjectured in 1937 [113]. With the development of particle physics since that time and specifically the acceptance of baryon number as a good symmetry to understand observed nuclear phenomena, it is now commonly accepted that the neutron is not a Majorana fermion. However a tiny Majorana component to its mass that violates baryon number remains an intriguing possibility. The early history of other physics ideas related to n-$\bar{n}$ oscillations is briefly discussed in [114]. A more detailed exposure to neutron-antineutron oscillation can be found in Ref. [115].

There are many compelling reasons to think that fundamental particle interactions violate baryon number. Arguably, the most powerful reason is that generating the origin of the matter-anti-matter asymmetry in the universe requires that baryon number must be violated [4]. Cosmological inflation, which is strongly supported by astronomical data, implies that baryon number $\mathcal{B}$ was not conserved in the early universe [116, 117]. This argument depends on the observed magnitude of the baryon asymmetry of the universe but not on a mechanism of its generation. Other reasons including grand unified theories, has been addressed in the overview section.

Once we accept the possibility that baryon number is not a good symmetry of nature, there are many questions that must be explored to decide the nature of physics associated with $\mathcal{B}$-violation: Is $\mathcal{B}$ a global or local symmetry? Does baryon number occur as a symmetry by itself or does it appear in combination with lepton number, $\mathcal{L}$, i.e. $\mathcal{B}$ - $\mathcal{L}$, as the Standard Model would suggest? What is the scale of baryon number violation and the nature of the associated physics that is responsible for it? For example, is this physics characterized by a mass scale not too far above the TeV scale, so that it can be probed in experiments already searching for new physics in colliders as well as low energy rare processes? Are the details of the physics responsible for baryon-number violation such that they can explain the origin of matter?

Proton decay searches probe baryon number violation due to physics at a grand unified scale of $\sim 10^{15} - 10^{16}$ GeV. In contrast, the baryon-number violating process of n-$\bar{n}$ oscillation, where a free neutron spontaneously transmutes itself into an anti-neutron, has very different properties and probes quite different physics. The process violates baryon number by two units and is caused by operators that have mass dimension nine so that it probes new physics at mass scales $\sim$TeV and above. Therefore it can be probed by experiments searching for new physics at this scale. It may also be deeply connected to the possibility that neutrinos may be Majorana fermions, a natural expectation. A key question for experiments is whether there are theories that predict n-$\bar{n}$ oscillations at a level that can be probed in currently available facilities such as reactors or in contemplated ones such as Project X, with intense neutron fluxes. Equally important are the resulting constraints on physics beyond the Standard Model if no signal appears after the free-neutron oscillation time is improved by two orders of magnitude above the current limit of 0.86×10^8 s [38].

13.4.2 Some Background Concerning Baryon Number Violation

Early on, it was observed that in a model with a left-right symmetric electroweak group, $G_{LR} = \mathrm{SU}(2)_L \otimes \mathrm{SU}(2)_R \otimes \mathrm{U}(1)_{B-L}$, baryon and lepton numbers in the combination $\mathcal{B}$ - $\mathcal{L}$ can be be gauged in an anomaly-free manner. The resultant $\mathrm{U}(1)_{B-L}$ can be combined with color SU(3) in an SU(4) gauge group [119], giving rise to the group $G_{422} = \mathrm{SU}(4) \otimes \mathrm{SU}(2)_L \otimes \mathrm{SU}(2)_R$ [119, 120, 121]. A higher degree of unification involved models that embed either the Standard Model gauge group $G_{SM} = \mathrm{SU}(3)_c \otimes \mathrm{SU}(2)_L \otimes \mathrm{U}(1)_Y$ or G_{422} in a simple group such as $SU(5)$ or $SO(10)$ [19, 39]. The motivations for grand unification theories are well-known and include the unification of gauge interactions and their couplings, the related explanation of the quantization of weak hypercharge and electric charge, and the unification of quarks and leptons. The unification of quarks and leptons in grand unified theories generically leads to the decay of the proton and the decay of neutrons that would otherwise be stably bound in nuclei. These decays typically obey the selection rule $\Delta\mathcal{B} = -1$ and $\Delta\mathcal{L} = -1$. However, the general possibility of a different kind of baryon-number violating process, namely the $|\Delta\mathcal{B}| = 2$ process of $n - \bar{n}$ oscillations, was suggested [23] even before the advent of GUTs. This was further discussed and studied after the development of GUTs in [24, 25] and in a number of subsequent models [122, 123, 124, 125, 126, 127, 128, 129, 130, 131, 26, 31, 33, 34, 35, 36, 37]. Recently, a number of models have been constructed that predict $n - \bar{n}$ oscillations at levels within reach of an improved search [130, 131, 31, 36].

13.4.3 General Formalism for Analysis of $n - \bar{n}$ Oscillations

Since the neutron and antineutron have opposite magnetic moments, one must account for the magnetic splittings that may be present between n and $\bar{n}$ states in an oscillation experiment. This motivates the following review of the formalism for the two level (n,$\bar{n}$) system and $n-\bar{n}$ oscillations in an external magnetic field [25].

The n and $\bar{n}$ interact with the external $\vec{B}$ field via their magnetic dipole moments, $\vec{\mu}_{n,\bar{n}}$, where $\mu_n = -\mu_{\bar{n}} = -1.9\mu_N$ and $\mu_N = e/(2m_N) = 3.15 \times 10^{-14}$ MeV/Tesla. Hence, the effective Hamiltonian matrix for the two-level $n - \bar{n}$ system takes the form

$$\mathcal{M}_{\mathcal{B}} = \begin{pmatrix} m_n - \vec{\mu}_n \cdot \vec{B} - i\lambda/2 & \delta m \\ \delta m & m_n + \vec{\mu}_n \cdot \vec{B} - i\lambda/2 \end{pmatrix}, \tag{13.6}$$

where m_n is the mass of the neutron, δm is the $\mathcal{B}$-violating potential coupling the n and $\bar{n}$ states, and $1/\lambda = \tau_n = 880.1$ s is the mean neutron lifetime.

The transition probability can be derived as $P(n(t) = \bar{n}) = \sin^2(2\theta)\, \sin^2[(\Delta E)t/2]\, e^{-\lambda t}$, where $\Delta E \simeq 2|\vec{\mu}_n \cdot \vec{B}|$ and $\tan(2\theta) = -\delta m/(\vec{\mu}_n \cdot \vec{B})$. In a free propagation experiment, the quasi-free condition must hold, such that $|\vec{\mu}_n \cdot \vec{B}|t << 1$. In this limit and also assuming that $t << \tau_n$, $P(n(t) = \bar{n}) \simeq [(\delta m)\, t]^2 = (t/\tau_{n-\bar{n}})^2$.

Then the number of $\bar{n}$'s produced by the $n - \bar{n}$ oscillations is given essentially by $N_{\bar{n}} = P(n(t) = \bar{n})N_n$, where $N_n = \phi T_{run}$, with ϕ the integrated neutron flux and T_{run} the running time. The sensitivity of the experiment depends in part on the product $t^2\phi$, so, with adequate magnetic shielding, one wants to maximize t, subject to the condition that $|\vec{\mu}_n \cdot \vec{B}|t << 1$.

13.4.3.1 $n - \bar{n}$ Oscillations in Matter

To put the proposed free propagation n-$\bar{n}$ oscillation experiment in perspective, it is appropriate to review limits that have been achieved in the search for $n - \bar{n}$ oscillations in nuclei. In 2002, the Soudan experiment reported a bound on the intranuclear transition time of $\tau_m > 0.72 \times 10^{32}$ yr (90% CL) [132] in ^{56}Fe. Using the relation $\tau_{n-\bar{n}} = \sqrt{\tau_m/R}$, where nuclear structure calculations provide the suppresion factor $R \simeq 1.5 \times 10^{-23}$ s^{-1}, this is equivalent to $\tau_{n-\bar{n}} \sim 1.3 \times 10^8$ s. In 2011, the Super-Kamiokande experiment reported a limit $\tau_m > 1.9 \times 10^{32}$ yr (90% CL) [133] in ^{16}O, yielding $\tau_{n-\bar{n}} \sim 3.5 \times 10^8$ s using the most recent value for the R parameter for ^{16}O [112]. The envisioned free neutron propagation experiment has the potential to improve substantially on these limits. Achieving sensitivities of $\tau_{n-\bar{n}} \sim 10^9$ s to 10^{10} s would be roughly equivalent to $\tau_m \simeq (1.6 - 3.1 \times 10^{33}$ yr$)(\tau_{n-\bar{n}}/10^9$ s$)^2$.

13.4.4 Operator Analysis and Estimate of Matrix Elements

At the quark level, the $n \to \bar{n}$ transition is $(udd) \to (u^c d^c d^c)$. This is mediated by six-quark operators $\mathcal{O}_i$, so the transition amplitude is characterized by an effective mass scale M_X and is expressed as

$$\delta m = \langle \bar{n} | H_{eff} | n \rangle = \frac{1}{M_X^5} \sum_i c_i \langle \bar{n} | \mathcal{O}_i | n \rangle. \tag{13.7}$$

Hence, $\delta m \sim \kappa \Lambda_{QCD}^6 / M_X^5$, where κ is a generic κ_i and $\Lambda_{QCD} \simeq 200$ MeV arises from the matrix element $\langle \bar{n} | \mathcal{O}_i | n \rangle$. For $M_X \sim$ few $\times 10^5$ GeV, one has $\tau_{n-\bar{n}} \simeq 10^9$ s.

The operators $\mathcal{O}_i$ must be color singlets and, for M_X larger than the electroweak symmetry breaking scale, also $\mathrm{SU}(2)_L \times \mathrm{U}(1)_Y$-singlets. An analysis of these (operators) was carried out in [126] and the $\langle \bar{n} | \mathcal{O}_i | n \rangle$ matrix elements were calculated in the MIT bag model. Further results were obtained varying MIT bag model parameters in [128]. These calculations involve integrals over sixth-power polynomials of spherical Bessel functions from the quark wavefunctions in the bag model. From the arguments above, it was found that

$$|\langle \bar{n} | \mathcal{O}_i | n \rangle| \sim O(10^{-4}) \text{ GeV}^6 \simeq (200 \text{ MeV})^6 \simeq \Lambda_{QCD}^6 \tag{13.8}$$

An exploratory effort has recently begun to calculate these matrix elements using lattice gauge theory methods [134]. Given that the mass scales probed by these measurements go well beyond the TeV scale, the fundamental impact of a result (whether or not oscillations are observed) and the availability of a variety of models predicting n-$\bar{n}$ at current sensitivity levels ($\tau_{n-\bar{n}} \sim 10^8$ s), there is strong motivation to pursue a higher-sensitivity $n - \bar{n}$ oscillation search experiment that can achieve a lower bound of $\tau_{n-\bar{n}} \sim 10^9 - 10^{10}$ s.

13.5 NNbarX: An Experimental Search for $n - \bar{n}$ Oscillations at Project X

Project X presents an opportunity to probe n-$\bar{n}$ transformation with free neutrons with an unprecedented improvement in sensitivity [135]. Improvements would be achieved by creating a unique facility, combining a high intensity cold neutron source *dedicated* to particle physics experiments with advanced neutron optics technology and detectors which build on the demonstrated capability to detect antineutron annihilation events with zero background. Existing slow neutron sources at research reactors and spallation sources possess neither the required space nor the degree of access to the cold source needed to take full advantage

of advanced neutron optics technology which enables a greatly improved free n-$\bar{n}$ transformation search experiment. Therefore, a dedicated source devoted exclusively to fundamental neutron physics, such as would be available at Project X, represents an exciting tool to explore not only n-$\bar{n}$ oscillations, but also other Intensity Frontier questions accessible through slow neutrons.

13.5.1 Previous Experimental Searches for $n - \bar{n}$ Oscillations

As mentioned in Sec. 13.4.3.1, the current best limit on n-$\bar{n}$ oscillations comes from the Super-Kamiokande experiment, which determined an upper-bound on the free neutron oscillation time of $\tau_{n-\bar{n}} > 3.5{\times}10^8$ s from n-$\bar{n}$ transformation in ^{16}O nuclei [112, 133]. An important point for underground water Cherenkov measurements is that these experiments are already limited in part by atmospheric neutrino backgrounds. Because only modest increments in detector mass over Super-Kamiokande are feasible and the atmospheric neutrino backgrounds will scale with the detector mass, dramatic improvements in the current limit will be challenging for such experiments.

Experiments which utilize free neutrons to search for n-$\bar{n}$ oscillations have a number of remarkable features. The basic idea for these experiments is to prepare a beam of slow (below room temperature) neutrons which propagate freely from the exit of a neutron guide to a distant annihilation target. During the time in which the neutron propagates freely, a $\mathcal{B}$-violating interaction can produce oscillations from a pure "n" state to one with an admixture of "n" and "$\bar{n}$" amplitudes. Antineutron appearance is sought through annihilation in a thin target, which generates several secondary pions seen by a tracking detector situated around the target. This signature strongly suppresses backgrounds. To observe this signal, the "quasi-free" condition must hold, in which the n and $\bar{n}$ are effectively degenerate. This creates a requirement for low pressures (below roughly 10^{-5} Pa for Project X) and very small ambient magnetic fields (between 1 and 10 nT for Project X) in order to prevent splittings between the neutron and antineutron from damping the oscillations. An improvement in sensitivity over the current free-neutron limit is available through the use of cutting-edge neutron optics, greatly increasing the neutron integrated flux and average transit time to the annihilation target.

The current best limit for an experimental search for free n-$\bar{n}$ oscillations was performed at the ILL in Grenoble in 1994 [38] (see Fig. 13-8). This experiment used a cold neutron beam from their 58 MW research reactor with a neutron current of $1.25{\times}10^{11} n/\mathrm{s}$ incident on the annihilation target and gave a limit of $\tau_{n-\bar{n}} > 0.86 \times 10^8$ s [38]. The average velocity of the cold neutrons was ~ 600 m/s and the average neutron observation time was ~ 0.1 s. A vacuum of $P \simeq 2 \times 10^{-4}$ Pa maintained in the neutron flight volume and a magnetic field of $|\vec{B}| < 10$ nT satisfied the quasi-free conditions for oscillations to occur. Antineutron appearance was sought through annihilation with a ~ 130 μm thick carbon film target which generated at least two tracks (one due to a charged particle) in the tracking detector with a total energy above 850 MeV in the surrounding calorimeter. In one year of operation the ILL experiment saw zero candidate events with zero background [38].

13.5.2 Overview of the NNbarX Experiment

A n-$\bar{n}$ oscillation search experiment at Project X (NNbarX) is conceived of as a two-stage experiment. The neutron spallation target/moderator/reflector system and the experimental apparatus need to be designed together in order to optimize the sensitivity of the experiment. The target system and the first-stage experiment can be built and start operation during the commissioning of the first-stage of Project X, which

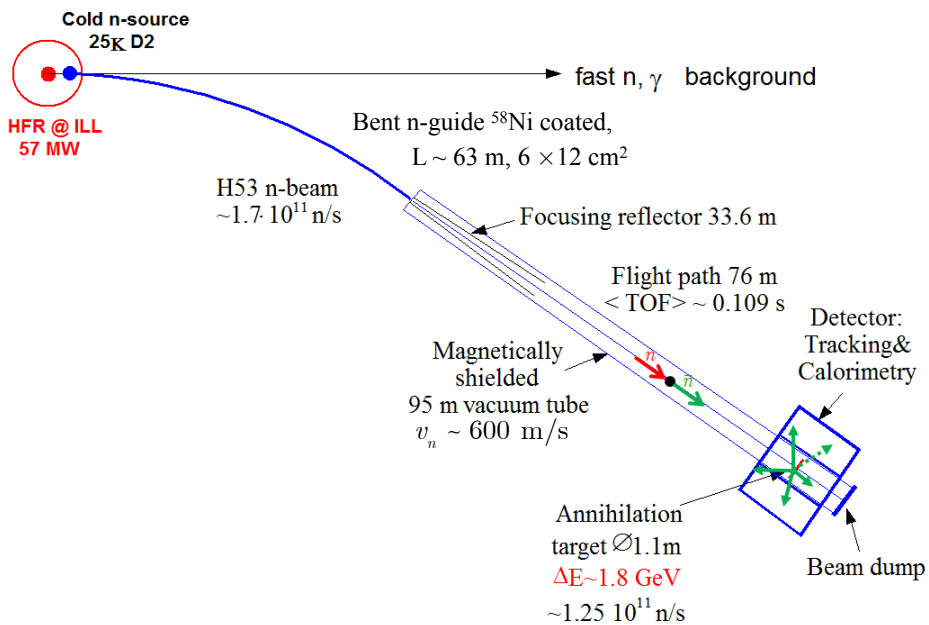

Figure 13-8. *Configuration of the horizontal n-$\bar{n}$ search experiment at ILL/Grenoble [38].*

is based on a 1 GeV proton beam Linac operating at 1 mA. The first-stage of NNbarX will be a horizontal experiment with configuration similar to the ILL experiment [38] performed in the 1990's, but employing modernized technologies which include an optimized slow neutron target/moderator/reflector system and an elliptical supermirror neutron focusing reflector. Our very conservative baseline goal for a first-stage experiment is a factor of 30 improvement of the sensitivity (probability of appearance) for n-$\bar{n}$ oscillations beyond the limits obtained in the ILL experiment [38]. This level of sensitivity would also surpass the n-$\bar{n}$ oscillation limits obtained in the Super-Kamiokande, Soudan-II, and SNO intranuclear searches [133, 132, 136]. In fact, although still in progress, our optimization studies indicate that this horizontal geometry is capable of improvements of a factor of 300 or more in 3 years of operation at Project X. A future, second stage of an NNbarX experiment can achieve higher sensitivity by exploiting a vertical layout and a moderator/reflector system which can make use of colder neutrons and ultracold neutrons (UCN) for the n-$\bar{n}$ search. This experimental arrangement involves new technologies that will require a dedicated R&D campaign, but the sensitivity of NNbarX should improve by another factor of ~ 100 with this configuration, corresponding to limits for the oscillation time parameter $\tau_{n-\bar{n}} > 10^{10}$ s. The increased sensitivity for n-$\bar{n}$ oscillations beyond the ILL experiment [38] provide a strong motivation to search for n-$\bar{n}$ oscillations as a part of Project X.

Intense beams of very low energy neutrons (meV) are available at facilities optimized for condensed matter studies focused on neutron scattering. These sources may be based on high flux reactors such as the ILL or the High Flux Isotope Reactor (Oak Ridge) or on accelerator based spallation sources such as SINQ (Switzerland) [137, 138], the SNS [139], or the JSNS in Japan [140]. Existing neutron sources are designed and optimized to serve a large number of neutron scattering instruments that each require beams with relatively small cross sectional areas. A fully optimized neutron source for an n-$\bar{n}$ oscillation experiment would require a beam having a very large cross section and large solid angle. There are no such beams at existing sources as these attributes would preclude them from providing the resolution necessary for virtually all instruments suitable for materials research. The creation of such a beam at an existing facility would require major modifications to the source/moderator/shielding configuration that would seriously impact the

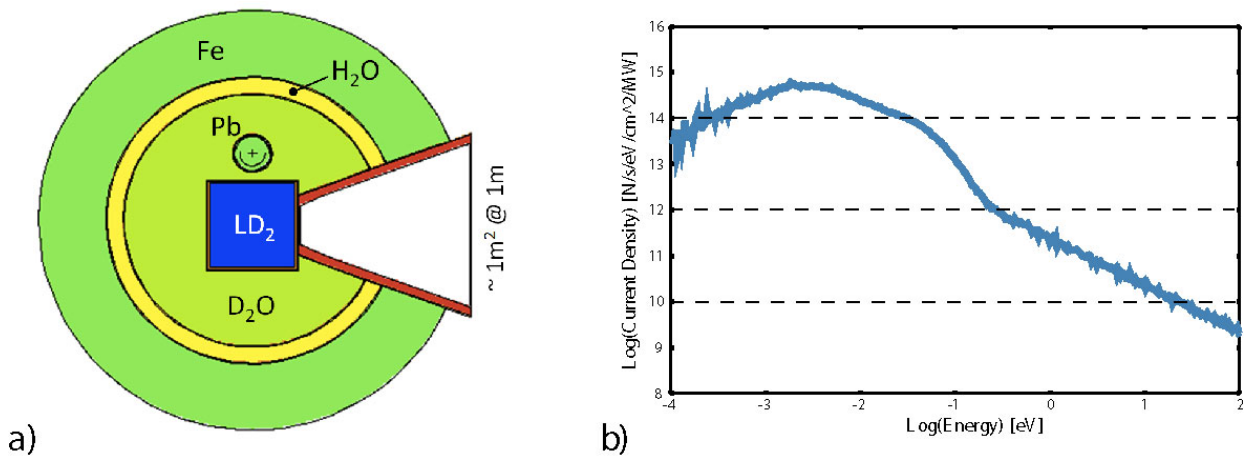

Figure 13-9. *a) Depiction of the initial NNbarX baseline cold neutron source geometry. b) MCNP simulation of the cold neutron spectrum entering the neutron optical system.*

its efficacy for neutron scattering. The reason there has been no improvement in the limit on free neutron n-$\bar{n}$ oscillations since the ILL experiment is that no substantial improvement is possible using existing sources.

The figure of merit for the sensitivity of a free n-$\bar{n}$ search experiment is $N_n \cdot t^2$, where N_n is the number of free neutrons observed and t is the neutron observation time (discussed in Sec.13.4.3). The initial intensity of the neutron source was determined in the ILL experiment by the brightness of the liquid deuterium cold neutron source and the transmission of the curved neutron guide. Although one expects the sensitivity to improve as the average velocity of neutrons is reduced, it is not practical to use very cold neutrons (< 200 m/s) with a horizontal layout for the n-$\bar{n}$ search due to effects of Earth's gravity, which will not allow free transport of very slow neutrons over significant distances in the horizontal direction.

Modest improvements in the magnetic field and vacuum levels reached for the ILL experiment would still assure satisfaction of the quasi-free condition for the horizontal experiment planned at Project X, but in our ongoing optimizations we will investigate limits of $|\vec{B}| \leq 1$ nT in the whole free flight volume and vacuum better than $P \sim 10^{-5}$ Pa in anticipation of the more stringent requirements for a vertical experiment. The costs of realizing these more stringent goals will be considered in our optimization of the experimental design.

The Project X spallation target system will include a cooled spallation target, reflectors and cold source cryogenics, remote handling, nonconventional utilities, and shielding. The delivery point of any high-intensity beam is a target which presents technically challenging issues for optimized engineering design, in that optimal neutron performance must be balanced by effective strategies for heat removal, radiation damage, remote handling of radioactive target elements, shielding, and other aspects and components of reliable safe operation. The NNbarX baseline design incorporates a spallation target core, which can be cooled by circulating water or heavy water and will be coupled to a liquid deuterium cryogenic moderator with optimized size and performance (see Fig. 13-9).

13.5.3 Increased Sensitivity of the NNbarX Experiment

A higher sensitivity in the NNbarX experiment compared to the previous ILL experiment [38], can be achieved by employing various improvements in neutron optics and moderation [142]. Conventional moderator designs

can be enhanced to increase the yield of cold neutrons through a number of neutronics techniques such as a reentrant moderator design [143], use of reflector/filters [144], supermirror reflectors [145], and high-albedo materials such as diamond nanoparticle composites [146, 147, 148]. Although potentially of high positive impact for an n-$\bar{n}$ experiment, some of these techniques are not necessarily suitable for multipurpose spallation sources serving a materials science user community (where sharply defined neutron pulses in time may be required, for example).

Supermirrors based on multilayer coatings can greatly increase the range of reflected transverse velocities relative to the nickel guides used in the ILL experiment. Supermirrors with $m = 4$, are now mass-produced and supermirrors with up to $m = 7$, can be manufactured [145], where m is the near-unity reflection above nickel. To enhance the sensitivity of the n-$\bar{n}$ search, the supermirrors can be arranged in the shape of a truncated focusing ellipsoid [149] (see Fig. 13-10a). The focusing reflector with a large acceptance aperture will intercept neutrons within a fixed solid angle and direct them by single reflection to the target. The cold neutron source and annihilation target will be located in the focal planes of the ellipsoid. The geometry of the reflector and the parameter m of the mirror material are chosen to maximize the sensitivity $N_n \cdot t^2$ for a given source brightness and a given moderator and annihilation target size. Elliptical concentrators of somewhat smaller scale have already been implemented for a variety of cold neutron experiments [150]. The plan to create a *dedicated* spallation neutron source for particle physics experiments creates a unique opportunity to position the NNbarX neutron optical system to accept a huge fraction of the neutron flux, resulting in large gains in the number of neutrons directed to the annihilation target. Such a strategy makes use of a large fraction of the available neutrons for a single beamline, so it would be incompatible with a typical multi-user materials science facility. Initial steps towards an optimized design have been taken, with an NNbarX source design similar to the SINQ source modeled and vetted vs. SINQ source performance (see Fig. 13-9), and a partially optimized elliptical neutron optics system shown in Fig. 13-10a.

MCNPX [151] simulation of the performance of the cold source shown in Fig. 13-9 produced a flux of cold neutrons emitted from the face of cryogenic liquid deuterium moderator into forward hemisphere with the spectrum shown in Fig. 13-9. Only a fraction of the integrated flux is accepted by the focusing reflector to contribute to the sensitivity at the annihilation target. Neutrons emitted from the surface of neutron moderator were traced through the detector configuration shown in Fig. 13-9 with gravity taken into account and with focusing reflector parameters that were adjusted by a partial optimization procedure. The flux of cold neutrons impinging on the annihilation detector target located at the distance L from the source was calculated after reflection (mostly single) from the focusing mirror. The time of flight to the target from the last reflection was also recorded in the simulation procedure. Each traced neutron contributed to the total sensitivity figure $N_n \cdot t^2$ that was finally normalized to the initial neutron flux from the moderator. Sensitivity as function of distance between neutron source and target is shown in Fig. 13-10(b). The simulation has several parameters that affect the sensitivity: emission area of the moderator, distance between moderator and annihilation target, diameter of the annihilation target, starting and ending distance for truncated focusing mirror reflector, semi-major axis of the ellipsoid ($L/2$), and the reflecting value "m" of the mirror. Sensitivity is a complicated functional in the space of these parameters. A vital element of our ongoing design work is to understand the projected cost for the experiment as a function of these parameters.

A sensitivity in NNbarX in units of the ILL experiment larger than 100 per year of running seems feasible from these simulations. Configurations of parameters that would correspond to even larger sensitivities are achievable, but for the baseline simulation shown in Fig. 13-10 we have chosen a set of parameters that we believe will be reasonably achievable and economical after inclusion of more engineering details than can be accommodated in our simulations to date. The optimal neutron optical configuration for an n-$\bar{n}$ search is significantly different from anything that has been built, so the impact on the sensitivity of cost and engineering considerations is not simple to predict at this early stage of the project. To demonstrate that the key sensitivity parameters predicted by these simulations do not dramatically depart from existing

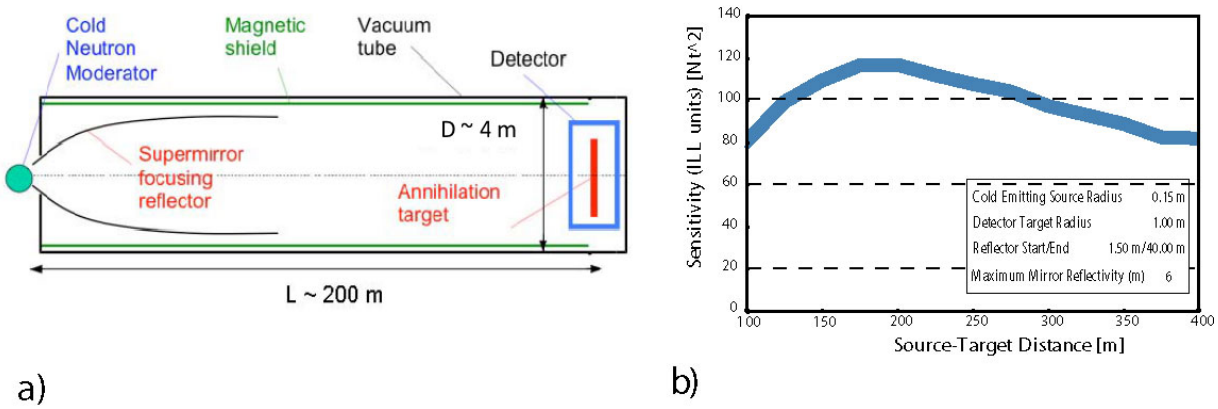

Figure 13-10. *a) Schematic diagram of a candidate NNbarX geometry, depicting the relative location of the cold neutron source, reflector, target, and annihilation detector. b) Calculation of the n-$\bar{n}$ oscillation sensitivity for a geometry similar to that in panel (a), where all parameters are fixed except for the source-target distance.*

engineering practice, we include Table 13-6, which shows the value of these same parameters at existing MW-scale spallation neutron sources for the source and optical parameters, and the ILL experiment for the overall length L.

Table 13-6. *Comparison of parameters in NNbarX simulations with existing practice.*

Parameter	Units	Used in Simulations	Existing MW Facility Value	References
Source brightness ($E < 400$ meV)	n/(s cm^2 sterad MW)	3.5×10^{12}	4.5×10^{12}	[140]
Moderator viewed area	cm^2	707	190	[140]
Accepted solid angle[1]	sterad	0.2	0.034	[141]
Vacuum tube length	m	200	100	[38]
^{12}C target diameter	m	2.0	1.1	[38]

[1] Note that the solid angle quoted from JSNS is the total for a coupled parahydrogen moderator feeding 5 neighboring beamlines (each of which would see a fifth of this value), whereas at NNbarX the one beam accepts the full solid angle.

13.5.4 Requirements for an Annihilation Detector

The target vacuum and magnetic field of 10^{-5} Pa and $|\vec{B}| < 1$ nT respectively is achievable with standard vacuum technology and with an incremental improvement on the ILL experiment through passive shielding and straight-forward active field compensation [38, 152, 153]. In the design of the annihilation detector, our strategy is to develop a state-of-the-art realization of the detector design used in the ILL experiment [38] (see Fig. 13-11a). The spallation target geometry of NNbarX introduces a new consideration in the annihilation detector design, because of the possible presence of fast neutron and proton backgrounds. These backgrounds were effectively eliminated from the ILL experiment, which produced fewer high energy particles in the reactor

source and eliminated the residual fast backgrounds using a curved guide system to couple the cold source to the n-$\bar{n}$ guide. For NNbarX, we utilize a strategy of integrating our shielding scheme for fast particles into the design of the source and beamline, and optimize the choice of tracker detectors to differentiate between charged and neutral tracks. The residual fast backgrounds at the detector are a strong function of the guide tube length, detector threshold, and pulse structure for the proton beam. In particular, if needed, a slow chopping of the proton beam (1 ms on, 1 ms off) will completely eliminate fast backgrounds at the expense of the integrated flux of neutrons on target.

In general, the n-$\bar{n}$ detector doesn't require premium performance, but due to relatively large size needs careful optimization of the cost. In the current NNbarX baseline experiment, a uniform carbon disc in the center of the detector vacuum region with a thickness of $\sim$ 100 μm and diameter $\sim$ 2 m would serve as an annihilation target. Carbon is useful as an annihilation target due to the low capture cross section for thermal neutrons $\sim$ 4 mb and high annihilation cross-section $\sim$ 4 kb. The fraction of hydrogen in the carbon film should be controlled below $\sim$ 0.1% to reduce generation of capture γ's. The detector should be built along a $\sim$ 4 m diameter vacuum region and cover a significant solid angle in θ-projection from $\sim$20° to 160° corresponding to the solid angle coverage of $\sim$94%. The wall should be have a thickness of $\sim$ 1.5 cm and be made of low-Z material (Al) to reduce multiple scattering for tracking and provide a low (n,γ) cross-section. Additional lining of the inner surface of the vacuum region with ^{6}LiF pads will reduce the generation of γ's by captured neutrons. The detector vacuum region is expected to be the source of $\sim 10^8$ γ's per second originating from neutron capture.

A tracker system should extend radially from the outer surface of the detector vacuum tube by $\sim$ 50 cm. It should provide rms $\leq$ 1 cm accuracy for annihilation vertex reconstruction to the position of the target in the θ-projection (compared to 4 cm in ILL experiment). This is a very important resource for the control of background suppression in the detector. Reconstruction accuracy in the ϕ-projection can be a factor of 3 - 4 lower. Relevant tracker technologies can include straw tubes, proportional and drift detectors. A system similar to the ATLAS transition radiation tracker (TRT) is currently under consideration for the tracking system. The ATLAS TRT has a measured barrel resolution of 118 μm and an end-cap resolution of 132 μm. The ATLAS TRT is capable of providing tracking for charged particles down to a transverse momentum of $p_T = 0.25$ GeV with an efficiency of 93.6%, but typically places a cut of $p_T > 1.00$ GeV due to combinatorics on the large number of tracks in collision events [154, 155, 156]. The time of flight (TOF) systems should consist of two layers of fast detectors (e.g. plastic scintillation slabs or tiles) before and after the tracker. With two layers separated by $\sim$50 cm - 60 cm, the TOF systems should have timing accuracy sufficient to discriminate the annihilation-like tracks from the cosmic ray background originating outside the detector volume.

The calorimeter will range out the annihilation products and should provide trigger signal and energy measurements. The average multiplicity of pions in annihilation at rest equals 5, so an average pion can be stopped in $\sim$20 cm of dense material (like lead or iron). For low multiplicity (but small probability) annihilation modes, the amount of material can be larger. The calorimeter configuration used in the ILL experiment, with 12 layers of Al/Pb interspersed with gas detector layers, might be a good approach for the calorimeter design. Detailed performance for the measurement of total energy of annihilation events and momentum balance in θ- and ϕ-projections should be determined from simulations. An approach using MINERνA-like wavelength shifting fibers coupled to scintillating bars is also being considered [157]. The cosmic veto system (CVS) surrounding the calorimeter should identify all cosmic ray background. Large area detectors similar to MINOS scintillator supermodules [158] might be a good approach to the configuration of the CVS. Possible use of timing information should be studied in connection with the TOF system. CVS information might not be included in the trigger due to high cosmogenic rates, particularly in the stage-one horizontal n-$\bar{n}$ configuration on the surface, but should be recorded for all triggers in the off-line analysis.

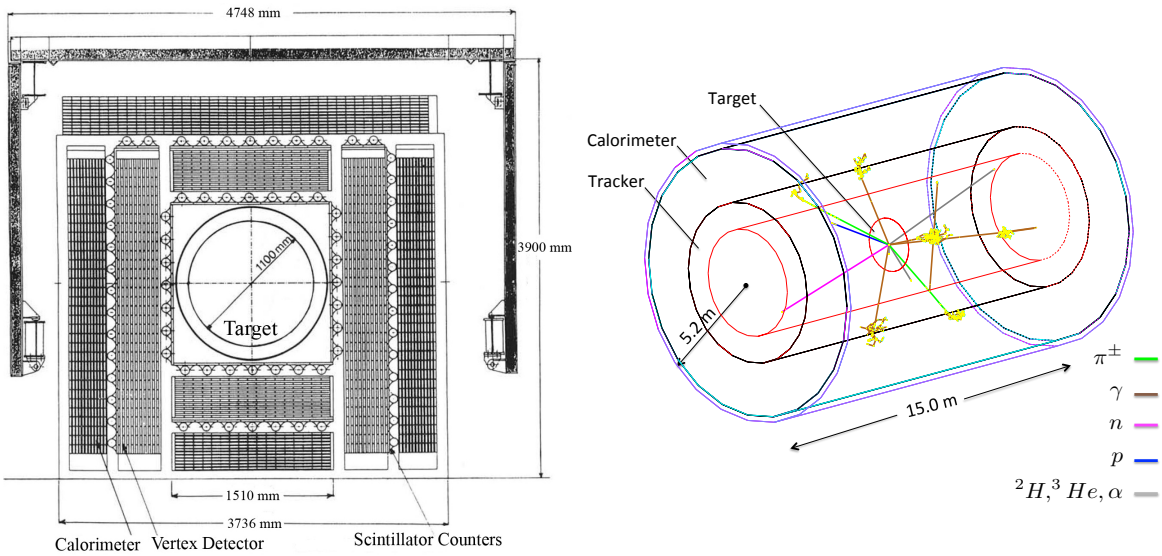

Figure 13-11. *a) Cross-sectional drawing of the ILL n-$\bar{n}$ annihilation detector [38]. b) Event display generated in our preliminary Geant4 [159] simulation for a $\pi^+\pi^-2\pi^0$ annihilation event in a generalized NNbarX detector geometry.*

13.5.5 NNbarX Simulation

Developing a detector model through simulation that allows us to reach our goal of zero background and optimum signal event detection efficiency is the primary goal of our simulation campaign, which is currently underway. We are using Geant 4.9.6 [159] to simulate the passage of annihilation event products through the annihilation detector geometry with concurrent remote development coordinated through GitHub [160]. A detailed treatment of n-$\bar{n}$ annihilation modes in ^{12}C is currently under development. According to a Super-Kamiokande simulation study, 90% of the n-$\bar{n}$ annihilation modes in ^{16}O are purely pionic, while the remaining 10% are captured in the $\pi^+\pi^-\omega$ mode [133], which we expect to be similar to the physics of NNbarX. The event generator for n-$\bar{n}$ annihilation modes in ^{12}C uses programs developed for the IMB experiment and Kamiokande II collaborations [161, 162] validated in part by data from the LEAR experiment [163]. The branching ratios for the n-$\bar{n}$ annihilation modes and fragmentation modes of the residual nucleus were taken from Ref. [133, 164, 165, 166]. The cross sections for the π-residual nucleus interactions were based on extrapolation from measured π-^{12}C and π-Al cross sections. Excitation of the $\Delta(1232)$ resonance was the most important parameter in the nuclear propagation phase. Nuclear interactions in the event generator include π and ω elastic scattering, π charge exchange, π-production, π-absorption, inelastic ω-nucleon scattering to a π, and ω decays inside the nucleus. Fig. 13-11b shows an event display from our preliminary Geant4 simulation of a $\pi^+\pi^-2\pi^0$ annihilation event in a detector geometry with a generalized tracker and calorimeter.

13.5.6 The NNbarX Research and Development Program

In October of 2012, the Fermilab Physics Advisory Committee strongly supported the physics of NNbarX and recommended that "R&D be supported, when possible, for the design of the spallation target, and for

the overall optimization of the experiment, to bring it to the level required for a proposal to be prepared." The NNbarX collaboration has identified several areas where research and development may substantially improve the physics reach of the experiment: target and moderator design, neutron optics optimization and the annihilation detector design. At the core of this activity is integrating models for the source, neutron optics and detectors into a useful tool for evaluating overall sensitivity to annihilation events and fast backgrounds, and developing a cost scaling model.

There exist a number of improvements for the target and moderator, which have already been established as effective and might be applied to our baseline conventional source geometry. For example, one can shift from a *cannelloni* target to a lead-bismuth eutectic (LBE) target [167], utilize a reentrant moderator design [143], and possibly use reflector/filters [144], supermirror reflectors [145], and high-albedo materials such as diamond nanoparticle composites [146, 147, 148]. At present, the collaboration envisions a program to perform neutronic simulations and possibly benchmark measurements on several of these possibilities, with high-albedo reflectors as a priority. Although the basic performance of neutron optics is established, optimizing the selection of supermirror technology for durability (*vs* radiation damage) and cost could have a very large impact on the ultimate reach of the experiment.

The collaboration is currently using the WNR facility at LANSCE to determine the detection efficiency and timing properties of a variety of detectors from 10 MeV to 800 MeV neutrons. Detectors under evaluation include proportional gas counters, straw tubes and plastic scintillators. Evaluating different available detector options and modernizing the annihilation detector should improve the background rejection capability and permit reliable scaling to more stringent limits for n-$\bar{n}$ oscillations. The main technical challenges for NNBarX are to minimize the cost of critical hardware elements, such as the large-area super-mirrors, large-volume magnetic shielding, vacuum tube, shielding of the high-acceptance front-end of the neutron transport tube, and annihilation detector components. These challenges will be addressed in the R&D phase for the NNBarX experiment.

13.5.7 Summary

Assuming beam powers up to 1 MW on the spallation target and that 1 GeV protons are delivered from the Project X linac, the goal of NNbarX will be to improve the sensitivity of an n-$\bar{n}$ search ($N_n \cdot t^2$) by at least a factor 30 (compared to the previous limit set in ILL-based experiment [38]) with a horizontal beam experiment; and by an additional factor of ~ 100 at the second stage with the vertical layout. The R&D phase of the experiment, including development of the conceptual design of the cold neutron spallation target, and conceptual design and optimization of the performance of the first-stage of NNbarX is expected to take 2-3 years. Preliminary results from this effort suggest that an improvement over the ILL experiment by a factor of more than 100 may be realized even in this horizontal mode, but more work is needed to estimate the cost of improvements at this level. The running time of the first stage of NNbarX experiment is anticipated to be 3 years. The second stage of NNbarX will be developed depending upon the demonstration of technological principles and techniques of the first stage.

13.6 Conclusions

While yet to be seen, proton decay is an indispensable tool for probing Nature at truly high energies. It remains as the missing piece of evidence for grand unification. The dramatic meeting of the three gauge couplings at a scale of about 2×10^{16} GeV, which is found to occur in the context of low energy supersymmetry,

and the tiny neutrino masses as observed in the neutrino oscillation experiments, lend strong support to the idea of supersymmetric grand unification. Moreover, grand unified theories that are in accord with the observed masses and mixings of all fermions, including neutrinos, typically predict proton lifetimes within a factor of five to 10 of current Super-Kamiokande limits. This is why an improved search for proton decay is now most pressing. This can only be done with a large detector built deep underground. Such a detector, coupled to a long-baseline intense neutrino beam (as would be available from Fermilab), can simultaneously sensitively study neutrino oscillations so as to shed light on neutrino mixing parameters, mass-ordering, and most importantly CP violation in the neutrino system. And it can help efficiently study supernova neutrinos. In short, such a detector would have a unique multi-purpose value with high discovery potential in all three areas. Building such a large underground detector coupled to a long-baseline neutrino beam in the US, in a timely fashion, would not only probe a set of fundamental issues in physics, but would enable the US to assume a leadership position by having a stellar facility that would be an asset to the world as a whole.

Neutron–antineutron oscillations probe a different sector with baryon number violation satisfying the selection rule $|\Delta\mathcal{B}| = 2$. Discovery of $n - \overline{n}$ oscillations in the next generation experiments would have a profound impact on the physics beyond the Standard Model. It may also suggest new low scale mechanisms of generating baryon asymmetry of the Universe. The potential to improve the oscillation probability by about four orders of magnitude provides a golden opportunity for a potential landmark discovery in science.

References

[1] H. Weyl, Z. Phys. **56**, 330 (1929) [Surveys High Energ. Phys. **5**, 261 (1986)].

[2] E.C.G. Stueckelberg, Helva. Phys. Acta. 11, 299 (1939).

[3] E.P. Wigner, Proc. Am. Phil. Soc. 93, 521 (1949).

[4] A. D. Sakharov, Pisma Zh. Eksp. Teor. Fiz. **5**, 32 (1967) [JETP Lett. **5**, 24 (1967)] [Sov. Phys. Usp. **34**, 392 (1991)] [Usp. Fiz. Nauk **161**, 61 (1991)].

[5] F. C. Adams and G. Laughlin, Rev. Mod. Phys. **69**, 337 (1997) [astro-ph/9701131].

[6] G. 't Hooft, Phys. Rev. Lett. **37**, 8 (1976).

[7] G. 't Hooft, Phys. Rev. D **14**, 3432 (1976) [Erratum-ibid. D **18**, 2199 (1978)].

[8] F. R. Klinkhamer and N. S. Manton, Phys. Rev. D **30**, 2212 (1984).

[9] V. A. Kuzmin, V. A. Rubakov and M. E. Shaposhnikov, Phys. Lett. B **155**, 36 (1985).

[10] M. Fukugita and T. Yanagida, Phys. Lett. B **174**, 45 (1986).

[11] S. Weinberg, hys. Rev. Lett. **43**, 1566 (1979).

[12] F. Wilczek and A. Zee, Phys. Rev. Lett. **43**, 1571 (1979).

[13] L. F. Abbott and M. B. Wise, Phys. Rev. D **22**, 2208 (1980).

[14] Y. B. Zeldovich, Phys. Lett. A **59**, 254 (1976).

[15] S. W. Hawking, D. N. Page and C. N. Pope, Phys. Lett. B **86**, 175 (1979).

[16] D. N. Page, Phys. Lett. B **95**, 244 (1980).

[17] J. R. Ellis, J. S. Hagelin, D. V. Nanopoulos and K. Tamvakis, Phys. Lett. B **124**, 484 (1983).

[18] J. C. Pati and A. Salam, Phys. Rev. Lett. **31**, 661 (1973); Phys. Rev. D **8**, 1240 (1974).

[19] H. Georgi and S. L. Glashow, Phys. Rev. Lett. **32**, 438 (1974).

[20] H. Georgi, H. R. Quinn and S. Weinberg, Phys. Rev. Lett. **33**, 451 (1974).

[21] E. Kearns, Talk presented at the ISOUP Symposium, Asilomar, CA, May (2013).

[22] F. Reines, C. L. Cowan and M. Goldhaber, Phys. Rev. **96**, 1157 (1954).

[23] V. Kuzmin, JETP Lett. **12**, 228 (1970).

[24] S. L. Glashow, Proc. Neutrino 79 Conf., Berge, **2**, 518 (1979).

[25] R. N. Mohapatra and R. E. Marshak, Phys. Rev. Lett. **44**, 1316 (1980) [Erratum-ibid. **44**, 1643 (1980)].

[26] K. S. Babu, R. N. Mohapatra and S. Nasri, Phys. Rev. Lett. **97**, 131301 (2006) [hep-ph/0606144].

[27] M. Claudson, L. J. Hall and I. Hinchliffe, Nucl. Phys. B **241**, 309 (1984).

[28] J. M. Cline and S. Raby, Phys. Rev. D **43**, 1781 (1991).

[29] K. Benakli and S. Davidson, Phys. Rev. D **60**, 025004 (1999) [hep-ph/9810280].

[30] D. J. H. Chung and T. Dent, Phys. Rev. D **66**, 023501 (2002) [hep-ph/0112360].

[31] B. Dutta, Y. Mimura and R. N. Mohapatra, Phys. Rev. Lett. **96**, 061801 (2006) [hep-ph/0510291].

[32] K. S. Babu, R. N. Mohapatra and S. Nasri, Phys. Rev. Lett. **98**, 161301 (2007) [hep-ph/0612357].

[33] K. S. Babu, P. S. Bhupal Dev and R. N. Mohapatra, Phys. Rev. D **79**, 015017 (2009) [arXiv:0811.3411 [hep-ph]].

[34] R. N. Mohapatra, J. Phys. G **36**, 104006 (2009) [arXiv:0902.0834 [hep-ph]].

[35] P. -H. Gu and U. Sarkar, Phys. Lett. B **705**, 170 (2011) [arXiv:1107.0173 [hep-ph]].

[36] K. S. Babu, P. S. Bhupal Dev, E. C. F. S. Fortes and R. N. Mohapatra, Phys. Rev. D **87**, 115019 (2013) [arXiv:1303.6918 [hep-ph]].

[37] J. M. Arnold, B. Fornal and M. B. Wise, Phys. Rev. D **87**, 075004 (2013) [arXiv:1212.4556 [hep-ph]].

[38] M. Baldo-Ceolin, P. Benetti, T. Bitter, F. Bobisut, E. Calligarich, R. Dolfini, D. Dubbers and P. El-Muzeini *et al.*, Z. Phys. C **63**, 409 (1994).

[39] H. Georgi, in *Particles and Fields*, Ed. by C. Carlson (AIP, NY, 1975); H. Fritzsch and P. Minkowski, Annals Phys. **93** 193 (1975).

[40] P. Langacker, Phys. Rept. **72**, 185 (1981); S. Raby, *Grand Unified Theories*, in K. Nakamura *et al.* [Particle Data Group Collaboration], J. Phys. G G **37**, 075021 (2010); P. Nath and P. Fileviez Perez, Phys. Rept. **441**, 191 (2007).

[41] S. Dimopoulos and H. Georgi, Nucl. Phys. B **193**, 150 (1981).

[42] N. Sakai, Z. Phys. C **11**, 153 (1981).

[43] S. Dimopoulos, S. Raby and F. Wilczek, Phys. Rev. D **24**, 1681 (1981); W. J. Marciano and G. Senjanovic, Phys. Rev. D **25**, 3092 (1982); C. Giunti, C. W. Kim and U. W. Lee, Mod. Phys. Lett. A **6**, 1745 (1991); P. Langacker and M. X. Luo, Phys. Rev. D **44**, 817 (1991); U. Amaldi, W. de Boer and H. Furstenau, Phys. Lett. B **260**, 447 (1991).

[44] A. H. Chamseddine, R. L. Arnowitt, P. Nath, Phys. Rev. Lett. **49**, 970 (1982).

[45] L. Hall, J. Lykken, S. Weinberg, Phys. Rev.D **27**, 2359 (1983).

[46] R. Barbieri, S. Ferrara and C. A. Savoy, Phys. Lett. B **119**, 343 (1982).

[47] For a review see P. Nath, [hep-ph/0307123].

[48] N. Sakai and T. Yanagida, Nucl. Phys. B **197**, 533 (1982).

[49] S. Weinberg, Phys. Rev. D **26**, 287 (1982).

[50] J. Hisano, H. Murayama and T. Yanagida, Nucl. Phys. B **402**, 46 (1993) [hep-ph/9207279].

[51] H. Murayama and A. Pierce, Phys. Rev. D **65**, 055009 (2002) [hep-ph/0108104].

[52] B. Bajc, P. Fileviez Perez and G. Senjanovic, arXiv:hep-ph/0210374; I. Gogoladze and A. Kobakhidze, Phys. Atom. Nucl. **60**, 126 (1997) [Yad. Fiz. **60N1**, 136 (1997)] [hep-ph/9610389].

[53] H. Georgi and C. Jarlskog, Phys. Lett. B **86**, 297 (1979).

[54] K. S. Babu, B. Bajc and Z. Tavartkiladze, Phys. Rev. D **86**, 075005 (2012) [arXiv:1207.6388 [hep-ph]].

[55] Y. Aoki *et al.*, Phys. Rev. D **75**, 014507 (2007) [arXiv:hep-lat/0607002]; Y. Aoki *et al.* [RBC-UKQCD Collaboration], Phys. Rev. D **78**, 054505 (2008) [arXiv:0806.1031 [hep-lat]].

[56] D. Chang, R. N. Mohapatra, J. Gipson, R. E. Marshak and M. K. Parida, Phys. Rev. D **31**, 1718 (1985); R. N. Mohapatra and M. K. Parida, Phys. Rev. D **47**, 264 (1993) [hep-ph/9204234]; N. G. Deshpande, E. Keith and P. B. Pal, Phys. Rev. D **46**, 2261 (1993); S. Bertolini, L. Di Luzio and M. Malinsky, Phys. Rev. D **85**, 095014 (2012) [arXiv:1202.0807 [hep-ph]].

[57] D. G. Lee, R. N. Mohapatra, M. K. Parida and M. Rani, Phys. Rev. D **51**, 229 (1995) [arXiv:hep-ph/9404238].

[58] K.S. Babu and S. Khan, to be published (2013).

[59] G. Altarelli and D. Meloni, JHEP **1308**, 021 (2013) [arXiv:1305.1001 [hep-ph]].

[60] K. S. Babu and R. N. Mohapatra, Phys. Rev. Lett. **70**, 2845 (1993) [hep-ph/9209215]; B. Bajc, G. Senjanovic and F. Vissani, Phys. Rev. Lett. **90**, 051802 (2003) [hep-ph/0210207]; H. S. Goh, R. N. Mohapatra and S. -P. Ng, Phys. Lett. B **570**, 215 (2003) [hep-ph/0303055]; C. S. Aulakh, B. Bajc, A. Melfo, G. Senjanovic and F. Vissani, Phys. Lett. B **588**, 196 (2004) [hep-ph/0306242]; T. Fukuyama, A. Ilakovac, T. Kikuchi, S. Meljanac and N. Okada, Eur. Phys. J. C **42**, 191 (2005) [hep-ph/0401213]; S. Bertolini, T. Schwetz and M. Malinsky, Phys. Rev. D **73**, 115012 (2006) [hep-ph/0605006]; K. S. Babu and C. Macesanu, Phys. Rev. D **72**, 115003 (2005) [hep-ph/0505200]; B. Dutta, Y. Mimura and R. N. Mohapatra, Phys. Rev. Lett. **100**, 181801 (2008) [arXiv:0712.1206 [hep-ph]]; C. S. Aulakh and S. K. Garg, Mod. Phys. Lett. A **24**, 1711 (2009) [arXiv:0710.4018 [hep-ph]].

[61] K. S. Babu and C. Macesanu, Phys. Rev. D **72**, 115003 (2005) [hep-ph/0505200].

[62] H. S. Goh, R. N. Mohapatra, S. Nasri and S. -P. Ng, Phys. Lett. B **587**, 105 (2004) [hep-ph/0311330].

[63] S. Dimopoulos and F. Wilczek, *Proceedings Erice Summer School*, ed. A. Zichichi (1981).

[64] K. S. Babu and S. M. Barr, Phys. Rev. D **50**, 3529 (1994) [hep-ph/9402291].

[65] V. Lucas and S. Raby, Phys. Rev. D **55**, 6986 (1997) [hep-ph/9610293].

[66] R. Dermisek and S. Raby, Phys. Lett. B **622**, 327 (2005) [hep-ph/0507045]; M. Albrecht, W. Altmannshofer, A. J. Buras, D. Guadagnoli and D. M. Straub, JHEP **0710**, 055 (2007) [arXiv:0707.3954 [hep-ph]].

[67] K. S. Babu, J. C. Pati and F. Wilczek, Phys. Lett. B **423**, 337 (1998) [hep-ph/9712307]; Nucl. Phys. B **566**, 33 (2000) [hep-ph/9812538].

[68] R. Dermisek, A. Mafi and S. Raby, Phys. Rev. D **63**, 035001 (2001) [hep-ph/0007213].

[69] K. S. Babu, J. C. Pati and Z. Tavartkiladze, JHEP **1006**, 084 (2010) [arXiv:1003.2625 [hep-ph]].

[70] K. S. Babu, J. C. Pati and Z. Tavartkiladze, to be published (2013).

[71] P. Nath and R. M. Syed, Phys. Rev. D **77**, 015015 (2008) [arXiv:0707.1332 [hep-ph]]; Phys. Rev. D **81**, 037701 (2010) [arXiv:0909.2380 [hep-ph]]; K. S. Babu, I. Gogoladze, P. Nath and R. M. Syed, Phys. Rev. D **72**, 095011 (2005) [hep-ph/0506312]; Phys. Rev. D **74**, 075004 (2006) [hep-ph/0607244]; P. Nath and R. M. Syed, Phys. Lett. B **506**, 68 (2001) [Erratum-ibid. B **508**, 216 (2001)] [hep-ph/0103165]; Nucl. Phys. B **618**, 138 (2001) [hep-th/0109116]; JHEP **0602**, 022 (2006) [hep-ph/0511172].

[72] B. Dutta, Y. Mimura and R. N. Mohapatra, Phys. Rev. Lett. **94**, 091804 (2005) [hep-ph/0412105]; Phys. Rev. D **72**, 075009 (2005) [hep-ph/0507319]; Phys. Rev. Lett. **100**, 181801 (2008) [arXiv:0712.1206 [hep-ph]]; Phys. Rev. D **82**, 055017 (2010) [arXiv:1007.3696 [hep-ph]].

[73] K. L. Chan, U. Chattopadhyay and P. Nath, Phys. Rev. D **58**, 096004 (1998) [arXiv:hep-ph/9710473].

[74] G. Lazarides, Q. Shafi and C. Wetterich, Nucl. Phys. B **181**, 287 (1981); S. M. Barr, Phys. Lett. B **112**, 219 (1982); T. E. Clark, T. K. Kuo and N. Nakagawa, Phys. Lett. B **115**, 26 (1982); C. S. Aulakh and R. N. Mohapatra, Phys. Rev. D **28**, 217 (1983).

[75] I. Dorsner and P. Fileviez Perez, Phys. Lett. B **625**, 88 (2005) [arXiv:hep-ph/0410198].

[76] P. Fileviez Perez, Phys. Lett. B **654**, 189 (2007) [arXiv:hep-ph/0702287]; P. Fileviez Perez, H. Iminniyaz and G. Rodrigo, Phys. Rev. D **78**, 015013 (2008) [arXiv:0803.4156 [hep-ph]].

[77] P. Nath, A. H. Chamseddine and R. L. Arnowitt, Phys. Rev. D **32**, 2348 (1985); T. Goto and T. Nihei, Phys. Rev. D **59**, 115009 (1999) [arXiv:hep-ph/9808255]; B. Bajc, P. Fileviez Perez and G. Senjanovic, Phys. Rev. D **66**, 075005 (2002) [arXiv:hep-ph/0204311].

[78] R. Dermisek and A. Mafi, Phys. Rev. D **65**, 055002 (2002) [hep-ph/0108139].

[79] M. U. Rehman, Q. Shafi and J. R. Wickman, Phys. Lett. B **688**, 75 (2010) [arXiv:0912.4737 [hep-ph]].

[80] K. S. Babu and R. N. Mohapatra, Phys. Rev. Lett. **109**, 091803 (2012) [arXiv:1207.5771 [hep-ph]].

[81] Y. Kawamura, Prog. Theor. Phys. **105**, 999 (2001) [hep-ph/0012125].

[82] L. J. Hall, Y. Nomura, T. Okui and D. Tucker-Smith, Phys. Rev. D **65**, 035008 (2002) [hep-ph/0108071].

[83] L. J. Hall and Y. Nomura, Phys. Rev. D **66**, 075004 (2002) [hep-ph/0205067].

[84] K. S. Babu, I. Gogoladze and K. Wang, Nucl. Phys. B **660**, 322 (2003) [hep-ph/0212245].

[85] H. M. Lee, S. Raby, M. Ratz, G. G. Ross, R. Schieren, K. Schmidt-Hoberg and P. K. S. Vaudrevange, Phys. Lett. B **694**, 491 (2011) [arXiv:1009.0905 [hep-ph]].

[86] For recent reviews, see, for example: H. Davoudiasl and R. N. Mohapatra, New J. Phys. **14**, 095011 (2012) [arXiv:1203.1247 [hep-ph]]; K. Petraki and R. R. Volkas, arXiv:1305.4939 [hep-ph].

[87] H. Davoudiasl, D. E. Morrissey, K. Sigurdson and S. Tulin, Phys. Rev. Lett. **105**, 211304 (2010) [arXiv:1008.2399 [hep-ph]].

[88] H. Davoudiasl, D. E. Morrissey, K. Sigurdson and S. Tulin, Phys. Rev. D **84**, 096008 (2011) [arXiv:1106.4320 [hep-ph]].

[89] N. Blinov, D. E. Morrissey, K. Sigurdson and S. Tulin, Phys. Rev. D **86**, 095021 (2012) [arXiv:1206.3304 [hep-ph]].

[90] For sample lattice results, with kinematics relevant to IND, see: Y. Aoki, E. Shintani and A. Soni, arXiv:1304.7424 [hep-lat].

[91] A. Pais, Phys. Rev. D **8**, 1844 (1973).

[92] J. C. Pati, A. Salam and J. A. Strathdee, Nuovo Cim. A **26**, 72 (1975); J. C. Pati, A. Salam and J. A. Strathdee, Phys. Lett. B **108**, 121 (1982).

[93] P. Fileviez Perez and M. B. Wise, JHEP **1108** (2011) 068 [arXiv:1106.0343 [hep-ph]].

[94] M. Duerr, P. Fileviez Perez and M. B. Wise, Phys. Rev. Lett. **110** (2013) 231801 [arXiv:1304.0576 [hep-ph]].

[95] J. Beringer *et al.* (Particle Data Group), Phys. Rev. D86, 010001 (2012), `http://pdg.lbl.gov/2012/listings/rpp2012-list-p.pdf`

[96] S. Mine *et al.*, [K2K Collaboration], Phys. Rev. D **77**, 032003 (2008).

[97] M. Shiozawa, Preliminary results for the Super-Kamiokande Collaboration, presented at TAUP 2013, Asilomar, CA.

[98] H. Nishino *et al.* [Super-Kamiokande Collaboration], Phys. Rev. D **85**, 112001 (2012) [arXiv:1203.4030 [hep-ex]].

[99] K. Abe *et al.* [Super-Kamiokande Collaboration], arXiv:1305.4391 [hep-ex].

[100] K. Abe, T. Abe, H. Aihara, Y. Fukuda, Y. Hayato, K. Huang, A. K. Ichikawa and M. Ikeda *et al.*, arXiv:1109.3262 [hep-ex].

[101] T. Akiri *et al.* [LBNE Collaboration], arXiv:1110.6249 [hep-ex].

[102] M. Wurm *et al.* [LENA Collaboration], Astropart. Phys. **35**, 685 (2012) [arXiv:1104.5620 [astro-ph.IM]].

[103] A. Badertscher, A. Curioni, U. Degunda, L. Epprecht, S. Horikawa, L. Knecht, C. Lazzaro and D. Lussi *et al.*, arXiv:1001.0076 [physics.ins-det]. See also: `http://cds.cern.ch/record/1457543/` for LBNO LOI.

[104] L. Agostino, *et al.*, arXiv:1306.6865 [physics.ins-det]

[105] D. Beznosko, *et al.*, `http://if-neutrino.fnal.gov/whitepapers/yeh-sci.pdf`

[106] C. K. Jung, `arXiv:hep-ex/0005046`.

[107] D. B. Cline, F. Raffaelli and F. Sergiampietri, JINST **1**, T09001 (2006) [astro-ph/0604548].

[108] D.F. Cowen, Presentation at Intensity Frontier Workshop, Argonne National Laboratory,26 April, 2013. `https://indico.fnal.gov/contributionDisplay.py?contribId=118&sessionId=3&confId=6248`

[109] Y. Suzuki *et al.* [TITAND Working Group Collaboration], hep-ex/0110005.

[110] A. Bueno *et al.*, JHEP **0704**, 041 (2007), `arXiv:hep-ph/0701101`.

[111] C. B. Dover, A. Gal and J. M. Richard, Phys. Rev. D **27**, 1090 (1983).

[112] E. Friedman and A. Gal, Phys. Rev. D **78**, 016002 (2008) [arXiv:0803.3696 [hep-ph]].

[113] E. Majorana, Nuovo Cim. **14**, 171 (1937).

[114] L. B. Okun, arXiv:1306.5052 [hep-ph].

[115] K. Babu, S. Banerjee, D. V. Baxter, Z. Berezhiani, M. Bergevin, S. Bhattacharya, S. Brice and T. W. Burgess *et al.*, "Neutron-Antineutron Oscillations: A Snowmass 2013 White Paper," arXiv:1310.8593 [hep-ex].

[116] A. D. Dolgov, Phys. Rept. **222**, 309 (1992).

[117] A. D. Dolgov, Surv. High Energy Phys. **13**, 83 (1998).

[118] S. Raby, T. Walker, K. S. Babu, H. Baer, A. B. Balantekin, V. Barger, Z. Berezhiani and A. de Gouvea *et al.*, arXiv:0810.4551 [hep-ph].

[119] J. C. Pati and A. Salam, Phys. Rev. D **10**, 275 (1974) [Erratum-ibid. D **11**, 703 (1975)].

[120] R. N. Mohapatra and J. C. Pati, Phys. Rev. D **11**, 566 (1975).

[121] R. N. Mohapatra and J. C. Pati, Phys. Rev. D **11**, 2558 (1975).

[122] T. -K. Kuo and S. T. Love, Phys. Rev. Lett. **45**, 93 (1980).

[123] L. N. Chang and N. P. Chang, Phys. Lett. B **92**, 103 (1980).

[124] R. N. Mohapatra and R. E. Marshak, Phys. Lett. B **94**, 183 (1980).

[125] R. Cowsik and S. Nussinov, Phys. Lett. B **101**, 237 (1981).

[126] S. Rao and R. Shrock, Phys. Lett. B **116**, 238 (1982).

[127] S. P. Misra and U. Sarkar, Phys. Rev. D **28**, 249 (1983).

[128] S. Rao and R. E. Shrock, Nucl. Phys. B **232**, 143 (1984).

[129] S. J. Huber and Q. Shafi, Phys. Lett. B **512**, 365 (2001) [hep-ph/0104293].

[130] K. S. Babu and R. N. Mohapatra, Phys. Lett. B **518**, 269 (2001) [hep-ph/0108089].

[131] S. Nussinov and R. Shrock, Phys. Rev. Lett. **88**, 171601 (2002) [hep-ph/0112337].

[132] J. Chung, W. W. M. Allison, G. J. Alner, D. S. Ayres, W. L. Barrett, P. M. Border, J. H. Cobb and H. Courant *et al.*, Phys. Rev. D **66**, 032004 (2002) [hep-ex/0205093].

[133] K. Abe *et al.* [Super-Kamiokande Collaboration], arXiv:1109.4227 [hep-ex].

[134] M. I. Buchoff, C. Schroeder and J. Wasem, PoS LATTICE **2012**, 128 (2012) [arXiv:1207.3832 [hep-lat]].

[135] A. S. Kronfeld, R. S. Tschirhart, U. Al-Binni, W. Altmannshofer, C. Ankenbrandt, K. Babu, S. Banerjee and M. Bass *et al.*, arXiv:1306.5009 [hep-ex].

[136] M. Bergevin, PhD Thesis, "Search for Neutron-Antineutron Oscillations at the Sudbury Neutrino Observatory", University of Guelph, (2010).

[137] B. Blau et. al., Neutron News, **20**, 5 (2009).

[138] W. Fischer et. al., Physica B, **234**, 1202 (1997).

[139] T. E. Mason et. al., Physica B, **385**, 955 (2006).

[140] F. Maekawa et. al., Nucl. Inst. Meth. A, **620**, 159 (2010).

[141] T. Kai et. al., Nucl. Inst. Meth. A, **550**, 329 (2005).

[142] W. M. Snow *et al.* [proto-NNbar Collaboration], Nucl. Instrum. Meth. A **611**, 144 (2009).

[143] W. Mampe, P. Ageron, J. C. Bates, J. M. Pendlebury and A. Steyerl, Nucl. Instrum. Meth. A **284**, 111 (1989).

[144] M. Mocko and G. Muhrer, Nucl. Inst. Meth. A, **704**, 27 (2013).

[145] Industrial Manufacturer of supermirrors, http://www.swissneutronics.ch.

[146] V. V. Nesvizhevsky, E. V. Lychagin, A. Y. .Muzychka, A. V. Strelkov, G. Pignol and K. V. Protasov, Nucl. Instrum. Meth. A **595**, 631 (2008) [arXiv:0805.2634 [nucl-ex]].

[147] E. Lychagin et. al., Nucl. Inst. Meth. A, **611**, 302 (2009).

[148] E. V. Lychagin, A. Y. .Muzychka, V. V. Nesvizhevsky, G. Pignol, K. V. Protasov and A. V. Strelkov, Phys. Lett. B **679**, 186 (2009) [arXiv:0812.1635 [nucl-ex]].

[149] Y. Kamyshkov et. al., Proceedings of the ICANS-XIII meeting of the International Collaboration on Advanced Neutron Sources, p. 843 (1995).

[150] P. Boni, F. Grunauer and C. Schanzer, Nucl. Inst. Meth. A, **624**, 162 (2010).

[151] CNPX, http://mcnpx.lanl.gov/documents.html.

[152] Project X Physics Study (PXPS12), https://indico.fnal.gov/event/projectxps12, June (2012).

[153] W. Altmannshofer et. al., "Physics Opportunities with Stage 1 of Project X, http://www.fnal.gov/directorate/lbne-reconfiguration/ (2012).

[154] J. M. Stahlman, http://cds.cern.ch/record/1381599/files/ATL-INDET-PROC-2011-005.pdf.

[155] A. S. Boldyrev et. al., Instruments and Experimental Techniques, **55**, 323 (2012).

[156] R. Van Kooten, Indiana University, private communication (2013).

[157] K. McFarland, Nucl. Phys. B (Proc. Suppl.), **159**, 107 (2006).

[158] D. G. Michael et. al., Nucl. Inst. Meth. A, **596**, 190 (2008).

[159] Geant4: A Toolkit for the Simulation of the Passage of Particles through Matter, http://geant4.cern.ch.

[160] Github, https://github.com.

[161] T. W. Jones *et al.* [Irvine-Michigan-Brookhaven Collaboration], Phys. Rev. Lett. **52**, 720 (1984).

[162] M. Takita *et al.* [KAMIOKANDE Collaboration], Phys. Rev. D **34**, 902 (1986).

[163] E. S. Golubeva, A. S. Ilinov and L. A. Kondratyuk, "International Workshop on Future Prospects of Baryon Instability Search in p decay and n-$\bar{n}$ Oscillation Experiments", Vol. C96-03-28, p. 295 (1996).

[164] C. Berger *et al.* [Frejus Collaboration], Phys. Lett. B **240**, 237 (1990).

[165] Y. Fukuda *et al.* [Super-Kamiokande Collaboration], Nucl. Instrum. Meth. A **501**, 418 (2003).

[166] A. S. Botvina, A. S. Ilinov and I. N. Mishustin, Nucl. Phys. A **507**, 649 (1990).

[167] M. Wohlmuther et. al., "The Improved SINQ Target", 10th International Topical Meeting on Nuclear Application of Accelerators, April (2011).